ANNALS OF
BOTANY
Founded 1887

Secondary phloem diversity and evolution in Bignonieae (Bignoniaceae)

Marcelo R. Pace[1],*, Suzana Alcantara[3], Lúcia G. Lohmann[2] and Veronica Angyalossy[1]

[1]*Laboratório de Anatomia Vegetal, Departamento de Botânica, Instituto de Biociências, Universidade de São Paulo, Rua do Matão, 277, Cidade Universitária, CEP 05508-090, São Paulo, SP, Brazil,* [2]*Laboratório de Sistemática Vegetal, Departamento de Botânica, Instituto de Biociências, Universidade de São Paulo, Rua do Matão, 277, Cidade Universitária, CEP 05508-090, São Paulo, SP, Brazil and* [3]*Laboratório de Sistemática de Plantas Vasculares, Departamento de Botânica, Centro de Ciências Biológicas, Universidade Federal de Santa Catarina, CEP 88040-970, Florianópolis, SC, Brazil*
* For correspondence. E-mail marcelorpace@usp.br or marcelorpace@yahoo.com.br

● **Background and Aims** Phloem evolution has been explored in the literature across very broad scales, either for vascular plants as a whole or for major plant groups, such as the monocotyledons or the former dicotyledons. However, it has never been examined in a way that would elucidate evolutionary shifts leading to the diversification of phloem in single lineages. Therefore, the present study explores in detail the patterns of phloem evolution in the tribe Bignonieae (Bignoniaceae). This group represents a particularly good model for phloem studies since it is known to have a very conspicuous and diverse phloem.

● **Methods** A total of 19 phloem characters were coded in 56 species from all 21 genera currently recognized in the tribe Bignonieae, accounting for phloem wedge growth and for all the anatomical cell diversity encountered in the phloem. Phloem evolution was explored by reconstructing ancestral character states using maximum-likelihood assumptions with a time-calibrated molecular phylogeny for the group. Directionality and the effect of phylogenetic transformations in the current variation of quantitative traits and evolutionary correlations of selected discrete phloem traits were also tested under a maximum-likelihood approach.

● **Key Results** Individual phloem features are quite diverse in the tribe, but generally conserved within smaller clades. Contrasting phloem patterns were found when comparing major groups, with certain lineages having the phloem marked by a background of phloem fibres where all other cells are embedded, tangentially arranged sieve tubes and sieve-tubecentric parenchyma. In contrast, other lineages exhibited a scarcely fibrous phloem, regularly stratified phloem, sieve tube elements in radial or diffuse arrangement, and diffuse parenchyma. We found signals of directional evolution in fibre abundance and number of sieve areas, which increased in the '*Fridericia* and allies extended clade' and decreased in the 'Multiples of four extended clade', resulting in no signal of directionality when the whole Bignonieae was considered. In contrast, no indication of directional evolution was found for the axial parenchyma, either in single clades within Bignonieae or in the entire tribe. Positive correlation was found between sieve element length and both sieve plate type and the presence of a storied structure. Correlated evolution was also found between fibre abundance and several traits, such as sieve tube arrangement, sieve plate type, parenchyma arrangement, ray lignification and number of companion cells.

● **Conclusions** The secondary phloem of Bignonieae is extremely diverse, with sister lineages exhibiting distinct phloem anatomies derived from contrasting patterns of evolution in fibre abundance. Fibre abundance in the tribe has diversified in correlation with sieve tube arrangement, sieve tube morphology, number of companion cells and parenchyma type. The results challenge long-standing hypotheses regarding general trends in cell abundance and morphological cell evolution within the phloem, and demonstrate the need to expand studies in phloem anatomy both at a narrow taxonomic scale and at a broad one, such as to families and orders.

Key words: Phloem diversity, Bignonieae, Bignoniaceae, cambial variant, diversification, ancestral character state reconstructions, directional evolution, lianas, sieve elements, parenchyma, sclerenchyma, fibres, correlated evolution.

INTRODUCTION

Phloem is a vascular tissue of vital importance to plants since it carries all the photosynthates produced by the leaves and signalling molecules, such as mRNAs, to all plant parts. Formed by more than one cell type, the secondary phloem is considered a complex tissue composed of conducting cells (sieve elements), parenchyma (axial and radial) and generally sclerenchyma (fibres and/or sclereids). The general morphology of these cell types, their relative abundance in the tissue and their spatial organization are all extremely diverse, although they may be conserved within plant families, subfamilies and tribes (Roth, 1981). Thus, these characteristics have been useful in descriptions and used as a tool to identify large plant groups (Solereder, 1908; Zahur, 1959; Esau, 1969; Roth, 1981; Costa et al., 1997). Despite all this diversity, few studies have addressed when and how all these different phloem cell types and their spatial organization evolved.

Most studies on phloem diversity have been descriptive (Chattaway, 1953; Parameswaran and Liese, 1970; Roth, 1981; Angyalossy-Alfonso and Richter, 1991), and the only studies addressing phloem evolution were done on a large scale, considering either vascular plants as a whole (Hemenway, 1911, 1913; Zahur, 1959; Chavan *et al.*, 1983, 2000) or major plant groups, such as the monocotyledons (Cheadle and Whitford, 1941; Cheadle, 1948) or the former dicotyledons (Den Outer 1983, 1993). In these works, the authors mainly focused on characteristics of the sieve elements and their correlation with the relative abundance and morphology of other cell types, i.e. parenchyma and sclerenchyma. Based on the observation of numerous angiosperm plant families and the notion that phloem evolution should parallel xylem evolution, general 'trends of phloem evolution' have been proposed. Evolutionary trends proposed for sieve elements include a decrease in length, an increase in diameter and a gradual modification in the sieve plates from compound to simple sieve plates, generating more efficient conducting cells over time (Hemenway, 1913; Zahur, 1959; Esau, 1969; Den Outer, 1993). For parenchyma and sclerenchyma, a gradually increasing trend in abundance of parenchyma, but a decrease in abundance of fibres, has been suggested, the latter being replaced by sclereids (Zahur, 1959). Such hypotheses were mainly based on empirical correlations observed in sieve element morphology and sclerenchyma and parenchyma type and abundance, suggesting that sieve elements, parenchyma and sclerenchyma evolved together in the phloem (Zahur, 1959). However, no further explicit hypotheses have been proposed to add functional and/or adaptive explanations to these general evolutionary trends observed. However, these hypotheses have been challenged by authors such as MacDaniels (1918), who suggested that the morphologies of sieve tubes and the organization of other cells in the phloem would be more related to physiological (including plant maturity) and environmental aspects than phylogeny, but without providing explicit explanations on this matter. Despite these very broad analyses, to the best of our knowledge no studies have investigated phloem evolution on a narrower scale, in a way that would elucidate evolutionary shifts leading to the diversification of phloem in single lineages. Studies on a narrower scale would allow delimitation of the diversity present in lineages and specifically address directionality in the evolution of phloem characters and whether correlated evolution has occurred between these characters. Therefore, the present study explored in detail the patterns of phloem evolution in the tribe Bignonieae (Bignoniaceae). The family Bignoniaceae represents a particularly good model for phloem studies since it is known to have a very conspicuous (Roth, 1981) and diverse phloem (Pace *et al.*, 2011).

The tribe Bignonieae (Bignoniaceae, Lamiales) is a monophyletic group (Spangler and Olmstead, 1999; Lohmann, 2006; Olmstead *et al.*, 2009) and contains approximately half the species of the family, representing the most species-rich group of lianas in the Neotropics (~393 species in Bignonieae; Gentry, 1991; Lohmann, 2006). This group is particularly interesting anatomically for having a cambial variant characterized by the formation of four or multiples of four phloem wedges that furrow the xylem (Schenck, 1893; Dobbins, 1971; Pace *et al.*, 2009; Pace and Angyalossy, 2013) (Fig. 1), a synapomorphy of the tribe (Lohmann, 2006; Lohmann and Taylor, 2014). This
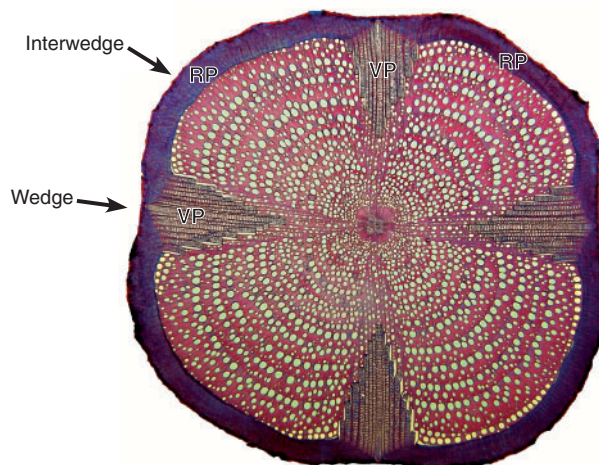

Fɪɢ. 1. Transverse section of *Tynanthus cognatus*. Wedges of variant phloem (VP) and interwedges with the regular phloem (RP).

cambial variant results in the formation of two distinct types of secondary phloem in the same stem: a regular phloem and a variant phloem (Fig. 1) (Solereder, 1908; Dobbins, 1971; Pace *et al.*, 2011). The two phloem types were shown to have several anatomical differences, including sieve tube element width, abundance of parenchyma, distribution of fibres and ray width (Pace *et al.*, 2011). Given these differences, it has been suggested that both phloem types in the tribe have evolved towards a division of labour, with the regular phloem assuming the function of storage and the variant phloem assuming the function of photosynthate conduction (Pace *et al.*, 2011), a phenomenon also reported in other plants in which a regular and variant phloem coexist (Carlquist, 2013).

Here, we conducted a detailed anatomical study of the variant phloem of Bignonieae and investigated its pattern of evolution within the tribe using a time-calibrated phylogeny as framework for the analyses (Lohmann *et al.*, 2013). We focus on (1) exploring the dynamics of phloem wedge growth; (2) exploring phloem diversity in Bignonieae by delimiting phloem characters and character states according to their anatomical variation; (3) exploring the distribution of characters across the phylogeny, their ancestral character states and evolutionary transitions within the tribe; (4) testing for directionality in the evolution of four continuous traits, including sieve element width, number of sieve areas per sieve plate and fibre and parenchyma abundance; and (5) testing for evolutionary correlation between specific pairs of characters involving sieve element dimensions and fibre abundance.

MATERIALS AND METHODS

Taxon sampling and anatomical procedure

We sampled the stems of 56 species representing all 21 genera currently recognized in Bignonieae (Lohmann and Taylor, 2014) and accounting for all the known anatomical diversity recorded for the tribe (Schenck, 1893; Dos Santos, 1995). Because the phylogenetic position of the monotypic *Callichlamys* is uncertain within Bignonieae (Lohmann, 2006;

Lohmann *et al.*, 2013), we only analysed the genus anatomically, and data for it were not incorporated in the phylogenetic analyses. Here we only consider the variant phloem of Bignonieae since the regular interwedge phloem has been explored elsewhere (Pace *et al.*, 2011). As the phloem is an extremely fragile tissue, most samples were collected in their natural habitat or from living collections (botanical gardens), with just a few specimens coming from wood collections (see Appendix). All specimens had their transverse section surfaces clear-cut to allow better penetration of the fixative, and they were immediately fixed in FAA 70 according to Berlyn and Miksche (1976) or Karnovsky (1965) while in the field. After a few days under vacuum, samples were transferred to a conserving solution of 50–70 % ethanol. Collected samples were standardized to have the same diameter (2 cm). This diameter is known to represent adult lianas already established in the canopy (Gerwing *et al.*, 2006), with fully developed stems (Pace *et al.*, 2009), and it is the most abundant diameter found for lianas growing in their natural habitats and already in their reproductive stage (Schnitzer *et al.*, 2006).

Before sectioning, all samples were softened in ethylenediamine for up to 4 d (Carlquist, 1982), rinsed in distilled water and gradually embedded in 1500 polyethylene glycol (Rupp, 1964). Samples were subsequently sectioned with a sliding microtome with the aid of an anti-tearing resin made of expanded polystyrene (foam) dissolved in butyl acetate (Barbosa *et al.*, 2010). Sections were double-stained in astra blue and safranin (Bukatsch, 1972), or sometimes with tannic acid, followed by ferric chloride and resorcin blue (lacmoid) whenever we wanted to better visualize the sieve plates (Cheadle *et al.*, 1953). Sections were then mounted in Canada balsam to make permanent slides. Furthermore, some samples were cut into cubes of 3 mm with phloem, cambium and xylem and embedded in Historesin® (Leica Microsystems). In this case, sections were made in a rotary microtome and stained in 0·05 % toluidine blue in glacial acetic buffer at pH 4·7 (O'Brien, 1964).

Phloem description, character coding and terminology

To properly analyse the development of phloem wedges and the variant phloem in Bignonieae, we performed detailed descriptions of their anatomy and development based on sequential sections of collected stems. The variation in anatomical traits among the analysed species was recorded as qualitative or quantitative traits, depending on their mode of variation. Sieve tube element length, sieve tube area, sieve tube diameter, percentage of phloem parenchyma and fibres in the phloem were calculated with ImageJ software, version 1·39 d (http://rsb.info.nih.gov/ij/), adopting the same procedures as described in Pace *et al.* (2011). The percentages were calculated using a grid of 0·05 mm^2 (50 000 μm^2) to calculate the total area occupied by each cell type, and at least four replications were made for each specimen analysed, and the average of all measurements was used to represent each species. The number of sieve areas was calculated in at least 20 sieve tube elements by manually counting the number of sieve areas in radial longitudinal sections of stems.

The anatomical terminology for phloem adopted here follows that proposed by Trockenbrodt (1990), Angyalossy-Alfonso and Richter (1991), Richter *et al.* (1996), Evert (2006) and the IAWA Committee list (2016) for most terms and Pace *et al.* (2009) for phloem wedges and interwedges. Phloem wedges are characterized as the regions produced by the activity of a variant cambium that produces less secondary xylem and more secondary phloem. Interwedges are characterized as the regions between phloem wedges, in which the cambium maintains regular activity (Pace *et al.*, 2009) (Fig. 1). As a result of variant cambial activity of the cambia within the phloem wedges, a variant phloem is formed (Fig. 1), while regular phloem is located in the interwedges (Fig. 1). Furthermore, we use the term 'sieve-tubecentric axial parenchyma' to refer to a sheath of phloem present around the sieve tubes whenever the variant phloem was characterized by a large amount of fibres forming a background tissue in which all other cell types are embedded (IAWA Committee, 2016).

Phylogenetic comparative analyses

To evaluate the patterns of phloem evolution, we performed statistical phylogenetic comparative analyses using a well-supported time-calibrated molecular phylogeny of the Bignonieae (Lohmann *et al.*, 2013). This phylogenetic framework was reconstructed based on a combined molecular dataset that included chloroplast (*ndhF*) and nuclear gene (*PepC*) sequences (Lohmann, 2006). Since a few species sampled in this study were not sampled in that phylogeny, we built a tree including the sampled species along with all the non-sampled species by collapsing them into the least inclusive node that represented genera or an existent subclade within the genera, in the most recent generic classification of the group (Lohmann and Taylor, 2014). In addition, we pruned the species that were not sampled in our anatomical study so that the final tree only contained the sampled taxa to which the relationships were known. This resulted in a totally resolved tree, which was then used for all the analyses performed here. We follow the clade names established in Lohmann *et al.* (2013): '*Fridericia* and allies clade', which includes the genera *Cuspidaria*, *Fridericia*, *Lundia*, *Tynanthus* and *Xylophragma*, and 'Multiples of four clade', which includes the genera *Amphilophium*, *Anemopaegma*, *Bignonia*, *Mansoa* and *Pyrostegia*. However, sometimes we use both clades with additions: the '*Fridericia* and allies clade', together with their sister clade formed by *Pachyptera*, *Pleonotoma* and *Manaosella*, was termed '*Fridericia* and allies extended clade', and the 'Multiples of four' + *Dolichandra* was termed 'Multiples of four extended clade'.

Characters were unordered in all analyses. Ancestral state reconstructions of discrete characters were performed in order to identify major state transitions along the phylogeny, using maximum-likelihood assumptions as implemented in Mesquite 2·75 (Maddison and Maddison, 2009). Continuous characters were optimized by parsimony, as implemented in Mesquite 2·75 (Maddison and Maddison, 2009).

We tested for directional evolution in the following traits: (1) sieve tube diameters; (2) number of sieve areas per sieve plates; (3) percentage of fibres; (4) percentage of axial parenchyma; and (5) percentage of axial parenchyma. All analyses were performed using the same phylogeny as that described above for the tribe Bignonieae (Lohmann *et al.*, 2013), as well as major subclades within the tribe. This procedure was done in order to

test whether individual clades within the phylogeny had a different evolutionary pattern when compared with the entire tribe. The analyses used the maximum-likelihood (ML) Pagel's (1999) test of models of evolution. This model approach is based on ML estimation for two alternative models of evolution, i.e. model A, which corresponds to the standard constant-variance (also called Brownian motion) random-walk model, and model B, which corresponds to the directional random-walk model, equivalent to model A, but with one additional parameter accounting for the directional rate of evolution of a trait. Model B detects any directional evolutionary signal. Likelihood ratio tests (LRTs) were performed to evaluate the best-fit model. In addition to the test for the best fit of model A (undirectional) or B (directional evolution), we also evaluate the effect of the tree-scaling parameters in the ML estimation in both model A and model B. These parameters are denoted κ, λ and δ and allow the respective tests of tempo (gradual versus punctuational evolution), phylogenetic associations and trait evolution (whether the phylogeny correctly predicts the covariance patterns of the traits) and mode (early versus late evolution; Pagel, 1999). We performed these analyses as implemented in BayesTraits V2 in accordance with the specifications in the companion manual.

Tests for correlated evolution between traits were performed for the following characters: length and type of sieve plates and features related to increase in fibre abundance, such as sieve plate type, arrangement of sieve tubes, fibre lignification and companion cell number. Since some of these features relate to continuous characters (e.g. sieve tube length), they were transformed into binary characters to allow the correlation analyses, and the characters and character states are presented in Table 3. Correlations were performed in Mesquite 2·75 (Maddison and Maddison, 2009), using Pagel's 1994 test of correlated character evolution, which uses an ML approach, and the LRT to evaluate models of correlated and independent evolution of any paired character states, using 1000 simulations (Midford and Maddison, 2006).

RESULTS

This study compared the secondary phloem of all 21 genera currently recognized in Bignonieae (Bignoniaceae) within a phylogenetic framework. We first explored the outline and development of phloem wedges, then the character and character states delimited for the secondary phloem in detail accompanied by analyses of ancestral character state reconstructions and analyses on directional evolution, and separately a test of correlated evolution between phloem traits. All the quantitative and qualitative data are summarized in Table 1, while the results of directionality analyses of continuous phloem traits are summarized in Table 2 and those of correlation analyses are summarized in Table 3.

Growth dynamics of phloem wedges

Here we explored two variable characters related to phloem wedges: their general outline and the diversity in the lignification status of the wide rays that border the

phloem wedges (hereafter termed 'limiting rays', a term coined by Schenck (1893)).

Phloem wedges types. When phloem wedges are first formed, they typically have straight lateral margins (Fig. 2A), and in some species it seems that the wedges remain straight throughout stem development (Fig. 2C). However, in many species the formation of lateral steps at both sides of the phloem wedges is common (Fig. 2B). These steps represent parts of a regular cambium on the sides of the phloem wedges that switch from regular to variant activity. According to the pattern these steps acquire, they may be symmetrically formed early in stem development, with each side of the phloem wedge having nearly the same pattern of steps (Fig. 2D), or they can form lateral steps at different times, resulting in an asymmetrical pattern on both sides of the wedge, with one side having more steps than the other (Fig. 2E). Straight margins kept throughout stem development are encountered solely in *Tanaecium* (Fig. 2C). Symmetrical phloem wedge steps are encountered in *Cuspidaria*, *Tynanthus* (these are sister groups; Fig. 2D) and *Manaosella*. All other genera display asymmetrical phloem wedge steps (Fig. 2E).

Formation of limiting rays The four to multiples of four equidistant regions of the phloem wedges are known not to grow in girth, since they lack anticlinal divisions (shown in Pace *et al.*, 2009). Therefore, while the stem thickens in Bignonieae, multiseriate rays are formed on the sides of the phloem wedges in order to accommodate secondary growth (Fig. 2C, arrows). The limiting rays appear as a single structure, but they are actually mixed in origin. The lateral outermost portion of the limiting rays is produced by the regular cambium at the sides of the phloem wedges (ray xylematic portion), while their innermost part is produced by the variant cambium from inside the phloem wedge (ray phloematic portion). The limiting rays are adjacent to the entire variant phloem and leave a conspicuous mark in the secondary xylem (Fig. 2C). Three groups can be distinguished, depending on the lignification status: (1) limiting ray cells only lignified next to the xylem and non-lignified in its phloematic portion (Fig. 3A); (2) limiting ray cells lignified next to both xylem and phloem, but with a row of non-lignified cells between the two parts (Fig. 3B); and (3) non-lignified limiting ray cells (Fig. 3C).

After the lateral steps are formed, some limiting rays start to be derived exclusively from the variant cambium (Fig. 2E). In the taxa in which the ray xylematic portion is lignified and the ray phloematic portion is non-lignified, the limiting rays will be exclusively non-lignified (except sometimes when crossing the fibre bands), since now all the limiting rays from the cambium outward will be exclusively phloematic (Fig. 2E).

Ancestral character state reconstructions unambiguously indicated that the ancestral condition of the tribe was the presence of limiting rays only lignified next to the xylem (Fig. 3D). In addition, a single origin of non-lignified limiting rays was observed in *Dolichandra* (Fig. 3D), and at least three independent origins of double-faced lignification were observed, once in *Adenocalymma salmoneum*, once in the '*Fridericia* and allies clade' (except for *Lundia*, with reversal to rays lignified only to
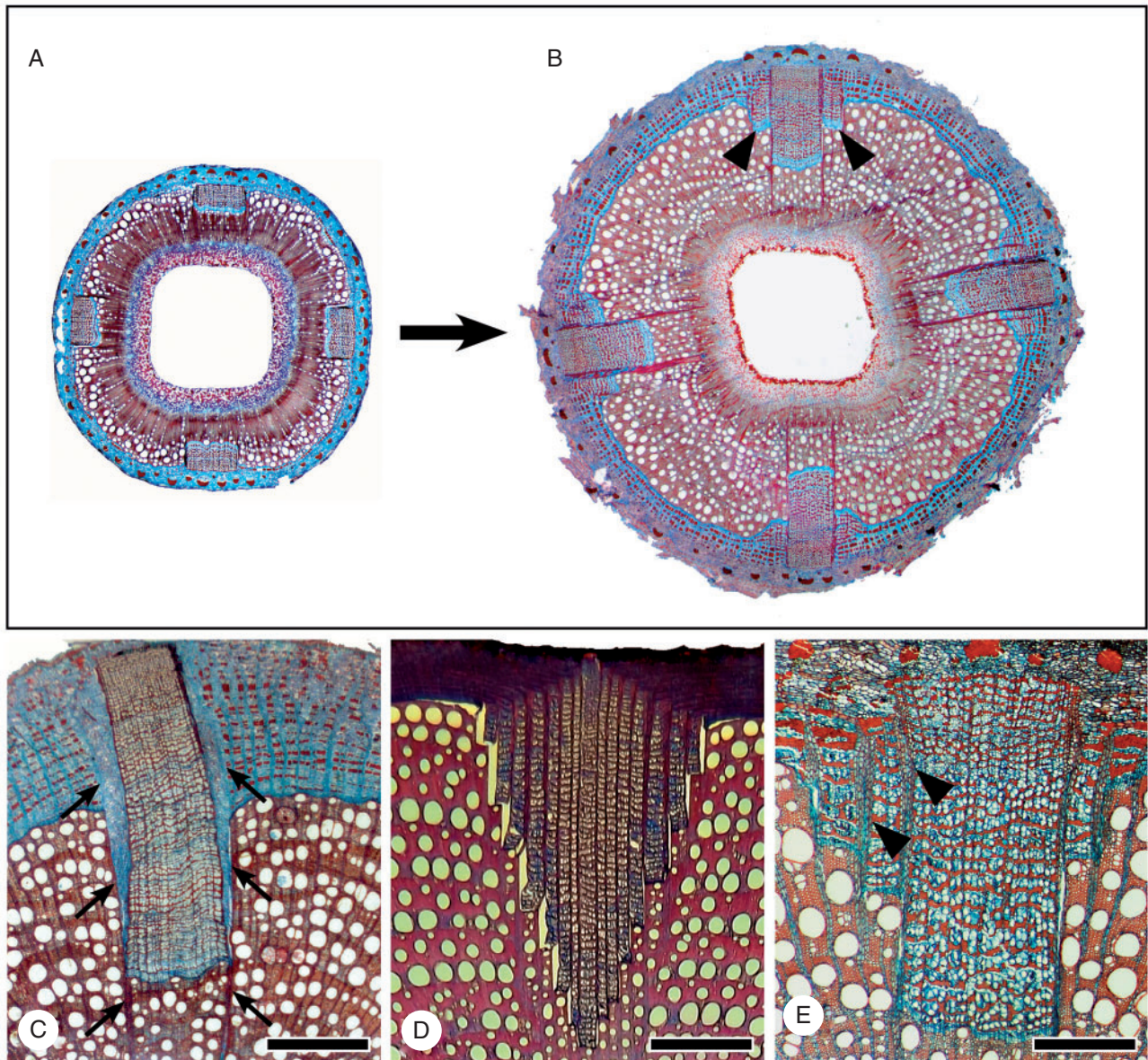
FIG. 2. Growth dynamics of phloem wedges. (A, B) Transverse sections of *Stizophyllum riparium*. (A) At the early stage of development, the phloem wedges have straight margins and no lateral steps. (B) At later stages of development, lateral steps are formed on the margins of phloem wedges (arrowheads), while the stem thickens. (C) Transverse section of *Tanaecium pyramidatum*: phloem wedges not forming lateral steps. Note the conspicuous multiseriate limiting rays on both sides of the phloem wedges (arrows). (D) Transverse section of *Tynanthus cognatus*: phloem wedges with early and regular formation of lateral steps. (E) Transverse section of *Fridericia samydoides*: phloem wedges with irregular formation of steps on each side of the phloem wedge. Scale bars = 3 mm.

the xylem face) and once in the clade formed by *Martinella* and *Stizophyllum* (Fig. 3D).

Phloem diversity: characters, ancestral state reconstructions and tests of directional evolution

Variant secondary phloem is located in phloem wedges (Fig. 1) and exhibits remarkable differences among genera. Nevertheless, here we first treat the features that are common to all genera and then discuss the variable characters, their ancestral character state reconstructions and the results of directional evolution.

Conducting phloem Sieve elements on the conducting phloem are generally grouped in multiples (Fig. 4A), but are sometimes solitary. The sieve elements are usually >500 μm in length, as seen in tangential section (Fig. 4B), and P-protein is frequently found as a slime plug at the sieve plates (Fig. 4B). Inside the wedges, rays are always uniseriate to biseriate and shorter than 1 mm in tangential section (Fig. 4B), except when these are limiting rays. When a ray borders a group of sieve elements, their companion cells are usually adjacent to the ray cells (Fig. 4C). Fibres in the fibre bands are more thick-walled than xylem fibres (Fig. 4A, arrows) and frequently exhibit a polylamellate structure. Furthermore, fibres possess a distinctive appearance, being square to rectangular in shape, as seen in
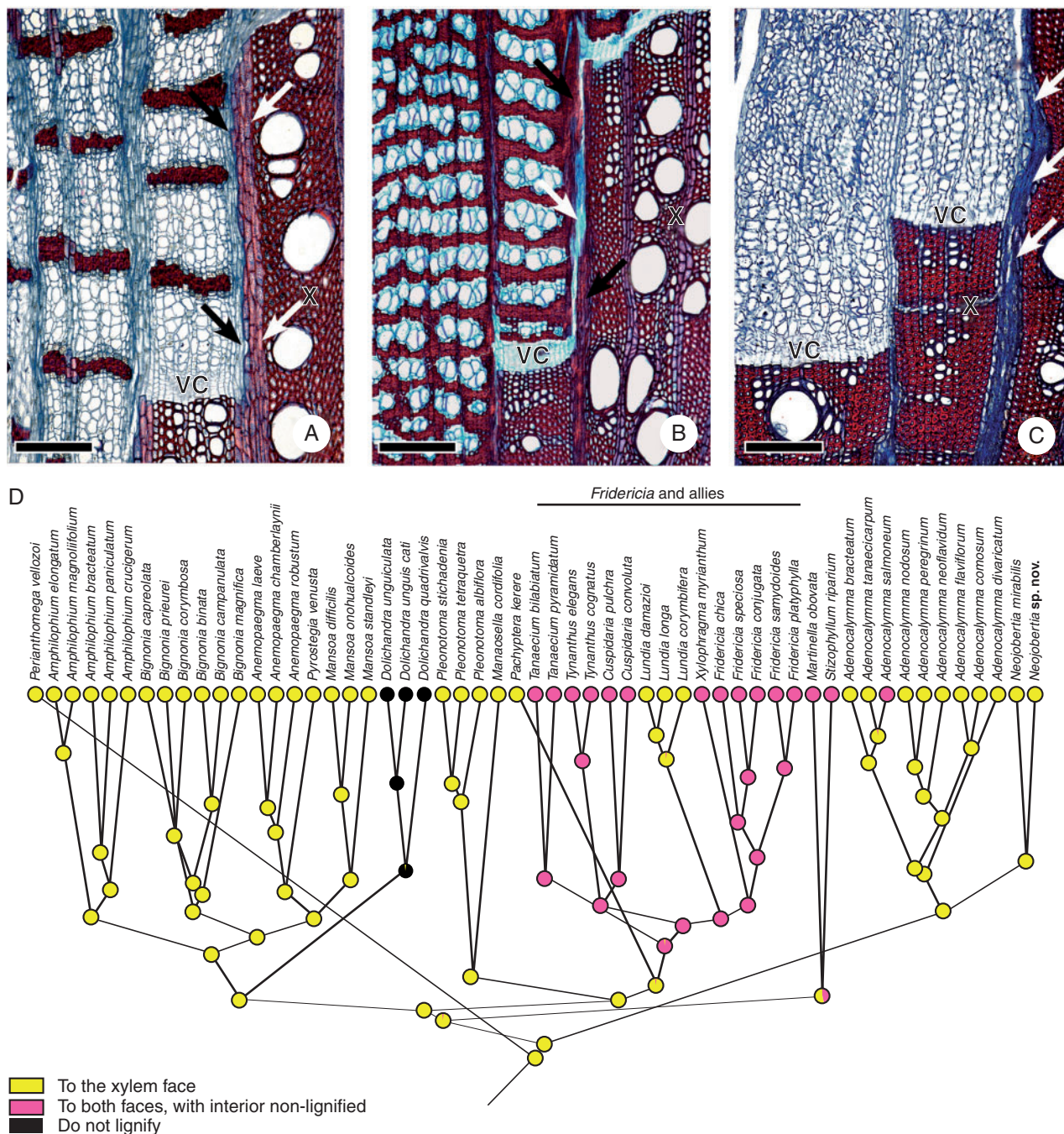
FIG. 3. Limiting ray lignification (variant portion). (A) Transverse section of *Pyrostegia venusta*. Limiting rays lignify only next to the xylem (white arrow), with its phloem portion non-lignified (black arrow). (B) Transverse section of *Tynanthus elegans*. Limiting rays are lignified next to the xylem and phloem (black arrows), with a row of cells remaining non-lignified in the middle portion (white arrow). (C) Transverse section of *Dolichandra unguiculata*. Limiting rays do not lignify, even in the xylem (arrows). (D) Ancestral character state reconstruction of limiting ray lignification. VC, variant cambium; X, xylem Scale bars = 200 μm.

transverse section (Fig. 4A). Radial sieve elements are rare, but were found in many species and may be widespread in the tribe.

Non-conducting phloem The cessation of function in variant phloem usually starts ~8–12 files of cells away from the cambium. The first sign of loss of function is seen as loss of protoplast in the companion cells, followed by accumulation of definitive callose at the sieve plates (Fig. 4D) and/or the

expansion of the phloem parenchyma cells. Ray dilatation is rarely seen, but when present it occurs in the outermost part of the wedge (Fig. 4E). A higher degree of crystal and starch accumulation is commonly observed in the non-conducting phloem (Fig. 4F) and sclerification of parenchyma cells is also common. In species in which the fibres are very abundant, no collapse of sieve tube elements is seen (Fig. 4E). On the other hand, for species with fewer fibres, total or partial collapse is evident (Fig. 5A).
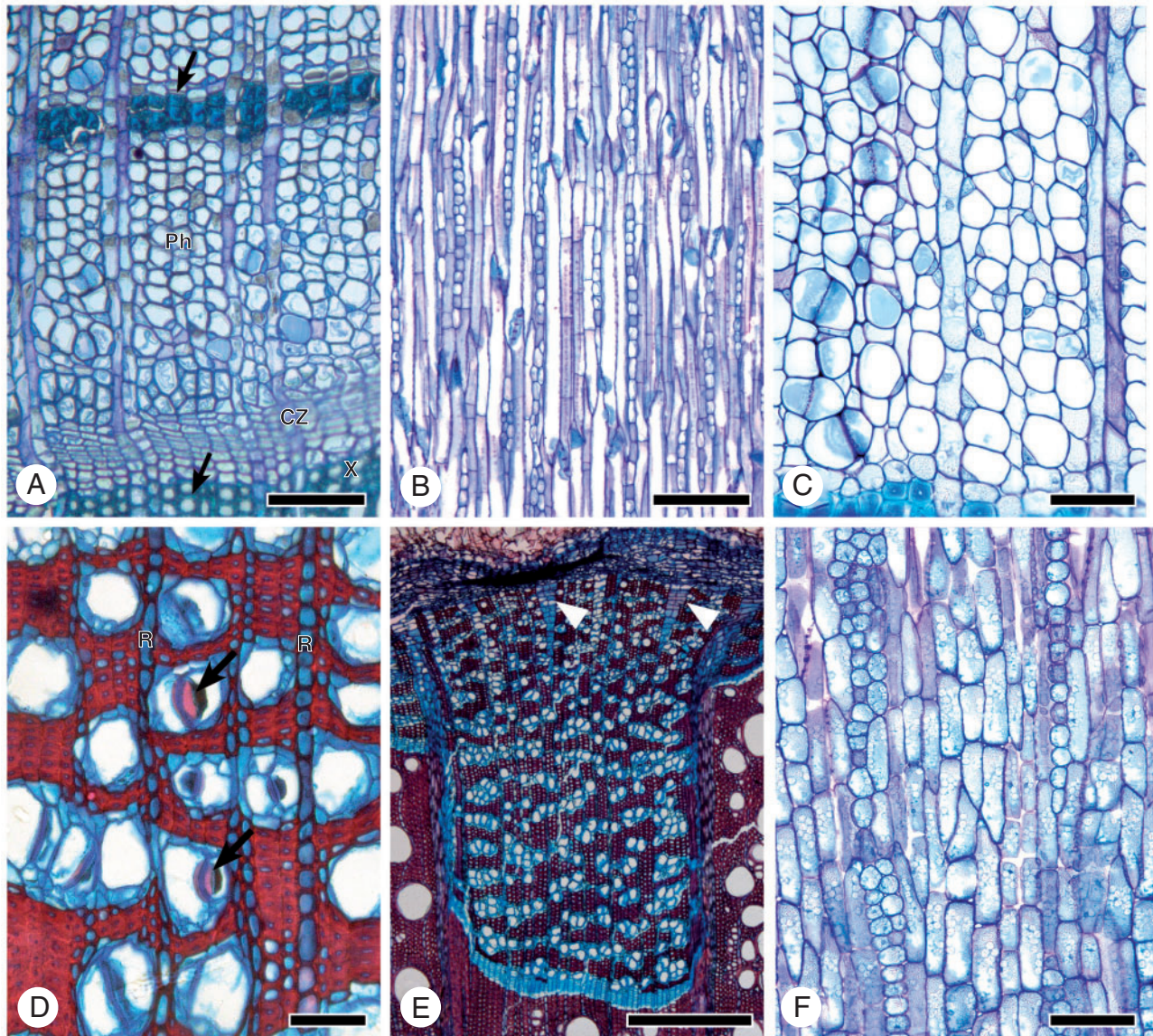
FIG. 4. Variant phloem, general aspects. (A–C) Conducting phloem of *Bignonia magnifica*. (A) Transverse section. Sieve tube elements grouped in multiples, fibre bands with rectangular-shaped fibres that are more thick-walled than the xylem fibres (arrows). Rays uniseriate to biseriate. (B) Longitudinal tangential section. Sieve tube elements longer than 500 µm and with conspicuous P-protein near the sieve plates forming a slime plug, rays uniseriate to biseriate and shorter than 1 mm. (C) Transverse section. Whenever a ray borders a group of sieve elements, their companion cells tend to lie adjacent to the ray cells. (D–F) Non-conducting phloem. (D) Transverse section of *Xylophragma myrianthum*. Massive definitive callose deposition at the sieve plates (arrows). (E) Transverse section of *Neojobertia* sp. nov. Rays rarely dilate in the variant phloem, and when they dilate it occurs only in the outermost part of the phloem wedges (arrowheads). (F) Longitudinal tangential section of *Bignonia magnifica*. Large amounts of starch accumulate in the parenchyma cells of the non-conducting phloem. Scale bars: (A, F) = 100 µm; (B) = 200 µm; (C–D) = 50 µm; (E) = 500 µm.

Variable characters of the variant phloem

Sieve tube width Sieve tube area, a continuous character, was calculated and analysed for directionality, revealing absence of directionality for this character within the tribe (Table 2). Furthermore, evolution of widths seems to have been independent of branch lengths, occurring in a punctuated fashion ($\kappa = 0$), independently of the phylogeny ($\lambda = 0$), and with most characters evolving close to the terminals (species-specific adaptation; $\delta = 3$).

Arrangement of sieve tube elements Three different types of arrangement can be found in Bignonieae: (1) predominantly diffuse (Fig. 5A), such as that found in *Amphilophium*, *Callichlamys* and *Manaosella*; (2) predominantly in radial multiples (Fig. 5B), such as that found in *Anemopaegma, Bignonia, Dolichandra, Mansoa, Martinella, Pachyptera, Perianthomega, Pyrostegia* and some *Adenocalymma*; and (3) predominantly in tangential multiples, such as that found in the entire 'Fridericia and allies clade' as well as in *Pleonotoma, Stizophyllum* and some *Adenocalymma* (Fig. 5C).
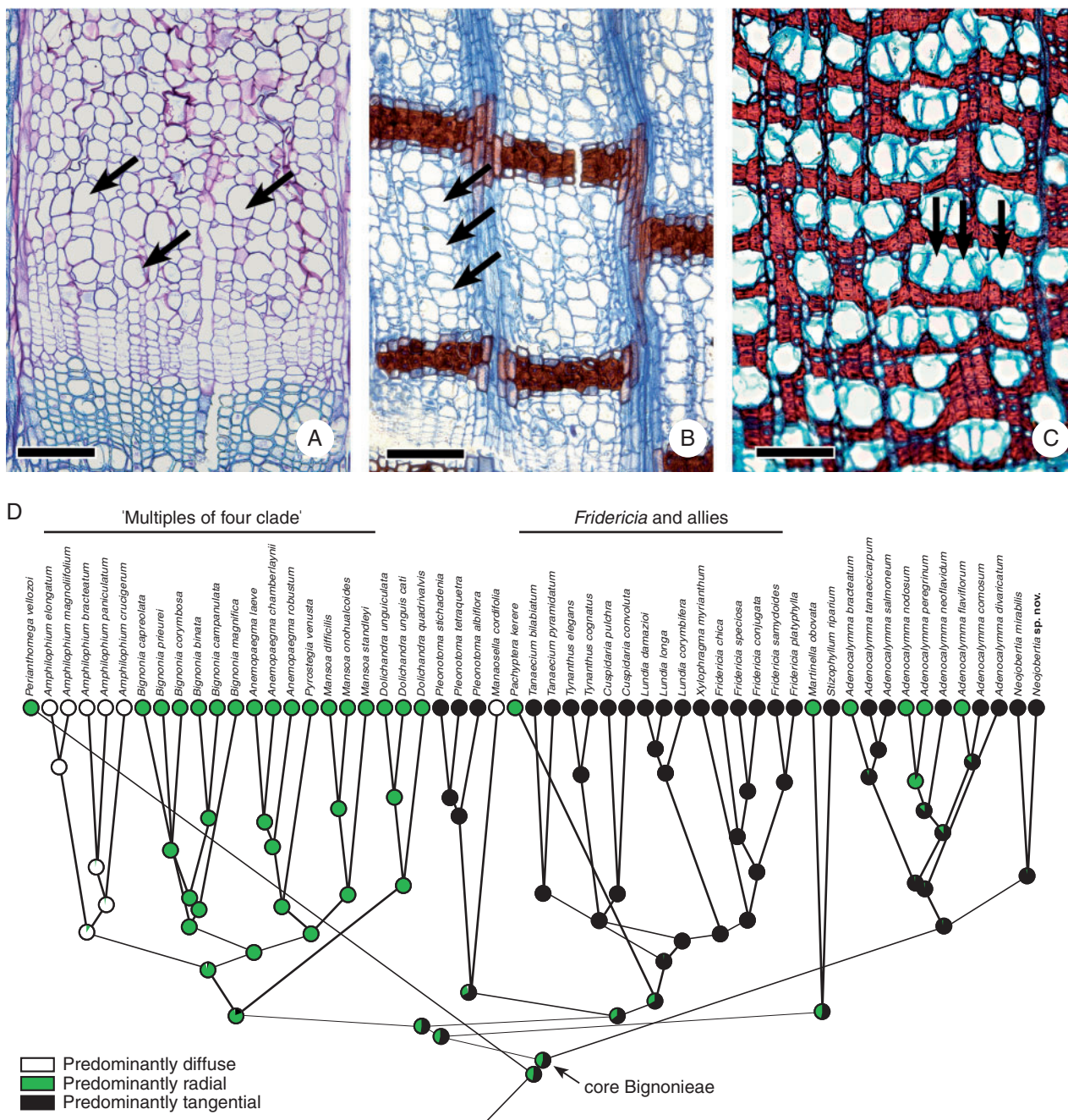
FIG. 5. Sieve tube arrangement in variant phloem. (A) Transverse section of *Amphilophium crucigerum*, with sieve tube elements diffusely arranged (arrows). (B) Transverse section of *Mansoa difficilis*, with sieve tube elements radially arranged (arrows). (C) Transverse section of *Cuspidaria convoluta*, with sieve tubes tangentially arranged (arrows). (D) Ancestral character state reconstruction of sieve tube element arrangement. Scale bars = 100 μm.

Ancestral character state reconstructions unambiguously reconstructed several character states at the most inclusive nodes (e.g. the 'Fridericia and allies clade' and the 'Multiples of four clade'; Fig. 5D), but ambiguously reconstructed the ancestral state of the tribe (Fig. 5D), assigning both radial and tangential arrangements with 50 % probability. The node for the core Bignonieae, which excludes *Perianthomega*, assigned 54 % probability that the ancestral state of this node had a tangential arrangement of sieve tubes (Fig. 5D). *Adenocalymma* was a very diverse genus in sieve tube arrangement, but its ancestral state was unambiguously reconstructed as having a tangential arrangement of the sieve tubes (Fig. 5D).

Sieve plates As seen in radial section, sieve tube elements have simple (Fig. 6A) to compound sieve plates (Fig. 6B–C). Compound sieve plates have few sieve areas (from three to five; Fig. 6B) or many sieve areas (>20; Fig. 6C), or even up to 40 sieve areas. Sieve tube elements with simple sieve plates are shorter than 500 μm, while those with compound sieve plates are longer than this (Fig. 6), an observation confirmed by the
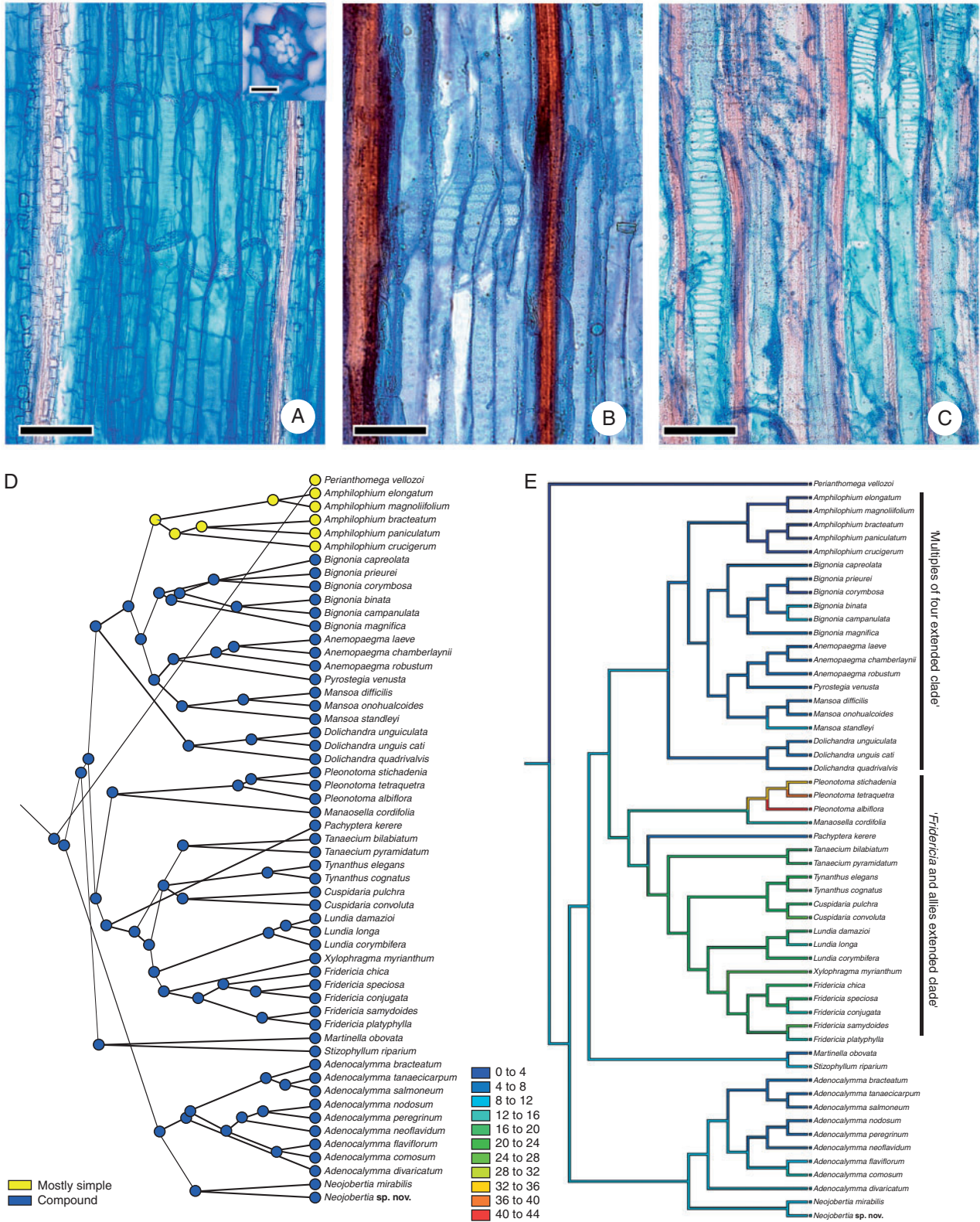
FIG. 6. Sieve plate type in variant phloem. (A) Longitudinal radial section of *Amphilophium crucigerum*. Sieve tube elements bearing simple sieve plates. Detail of a simple sieve plate with large sieve pores, as seen in transverse section. (B) Longitudinal radial section of *Bignonia campanulata*. Sieve tube elements bear compound sieve plates with few sieve areas. (C) Longitudinal radial section of *Fridericia samydoides*. Sieve tube elements bear compound sieve plates with many sieve areas. (D) Ancestral character state reconstruction of the sieve plate types. (E) Ancestral character state reconstruction of the average number of sieve areas per sieve plate. Scale bar = 50 μm.
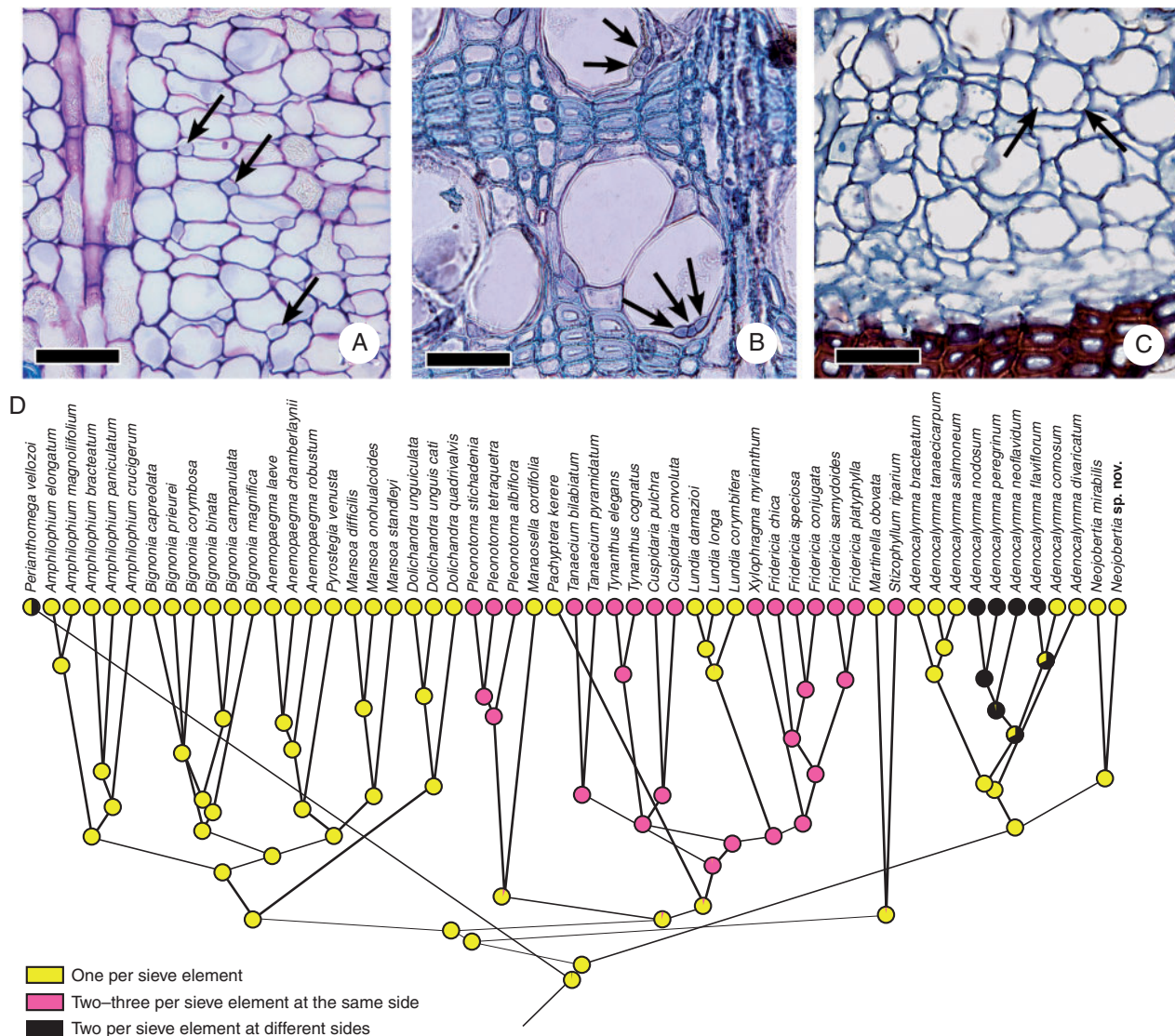
FIG. 7. Number of companion cells per sieve tube element in the variant phloem. (A) Transverse section of *Perianthomega vellozoi*. Sieve tube elements are accompanied by one companion cell (arrows). (B) Transverse section of *Tynanthus cognatus*. Sieve tube elements are accompanied by two or three companion cells lying at the same side of the sieve tube (arrows). (C) Transverse section of *Adenocalymma flaviflorum*. Sieve tube elements are accompanied by two companion cells, each at one corner of the sieve tube element (arrows). (D) Ancestral character state reconstruction of the number of companion cells per sieve tube element. Scale bars = 50 μm.

correlation analysis (see Correlation analyses section). Ancestral character state reconstructions unambiguously indicated compound sieve plates as the ancestral state in the tribe (Fig. 6D), with two independent origins for simple sieve plates, one in *Perianthomega* and another in *Amphilophium* (Fig. 6D).

When the average number of sieve areas (Table 1) was mapped as a continuous character, the ancestral condition for the tribe was reconstructed as having approximately three sieve areas per sieve plate. We found no signal of directional evolution when the tribe was considered as a whole. However, two major clades exhibited contrasting patterns. In the 'Multiples of four extended clade', sieve areas in the sieve plates decreased in number towards most terminal nodes (Fig. 6E; Table 2), with *Amphilophium* bearing mostly simple sieve plates and an ancestor inferred as bearing sieve plates with two sieve areas

(Fig. 6E). Tree-scaling parameters (Table 2) indicated that evolution in this clade was punctuational ($\kappa = 0{\cdot}0$), with a high phylogenetic signal ($\lambda = 0{\cdot}94$) and with most changes occurring early in the phylogeny (adaptive radiation; $\delta = 0{\cdot}54$).

In the clade that contains the '*Fridericia* and allies extended clade' (Fig. 6E), no directional evolution was detected in the number of sieve areas (Table 2). However, here we observed the genera with higher numbers of sieve areas per sieve plate, with the ancestor of *Manaosella* and *Pleonotoma* showing ~20 sieve areas per sieve plate and *Pleonotoma tetraquetra* with sieve plates having >30 sieve areas (Table 1). Tree-scaling parameters (Table 2) indicated that the evolution of this character was more conspicuous in the longer branches ($\kappa = 2{\cdot}28$), with high phylogenetic signal ($\lambda = 1{\cdot}0$) and occurring early in the phylogeny (adaptive radiation; $\delta = 0{\cdot}30$).
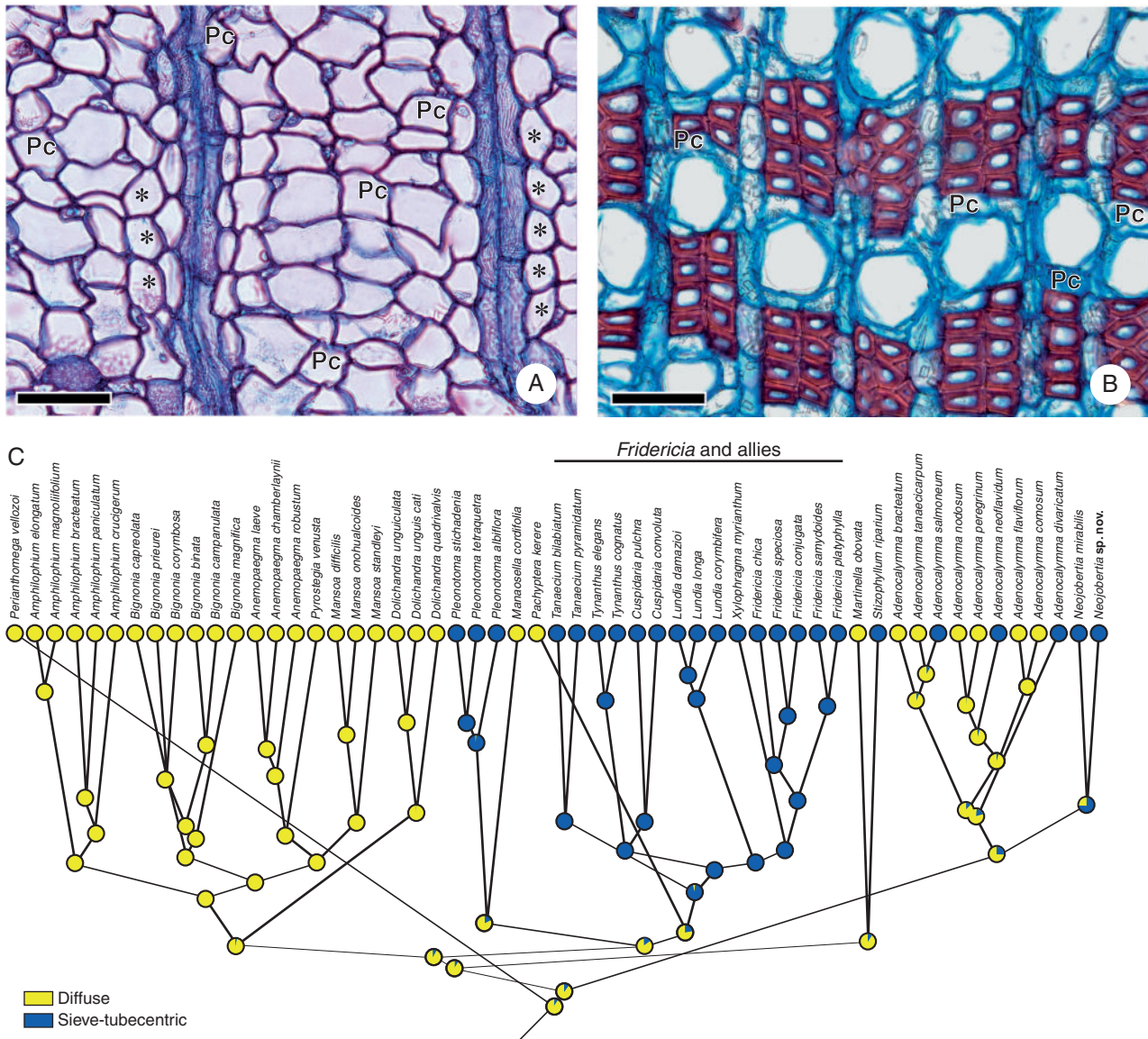
FIG. 8. Phloem parenchyma type in the variant phloem. (A) Transverse section of *Perianthomega vellozoi*. Diffuse phloem parenchyma. Radial rows were also found in the phloem (here shown with asterisks). (B) Transverse section of *Neojobertia* sp. nov. Sieve-tubecentric phloem parenchyma. (C) Ancestral character state reconstruction of phloem parenchyma type. Pc, axial parenchyma cell. Scale bar = 50 μm.

Companion cell Companion cells always accompany the sieve tube elements in one or more of their corners. However, the number and position of the companion cells are variable. In most Bignonieae a single companion cell is found per sieve tube element (Fig. 7A, D), while two or three companion cells lying at the same corner of the sieve tube element are found in *Cuspidaria*, *Fridericia*, some *Lundia*, *Pleonotoma*, *Stizophyllum*, *Tanaecium*, *Tynanthus* and *Xylophragma* (Fig. 7B) or, as in some *Adenocalymma*, two companion cells per sieve tube element, each lying on an opposite corner of the element (Fig. 7C). *Perianthomega* is polymorphic, sometimes having just one and sometimes two companion cells, lying at opposite sides of the sieve tube.

Ancestral character state reconstructions revealed that the ancestral state in the tribe was a single companion cell per sieve element (Fig. 7D), with at least three independent origins of

sieve tube elements with two or three companion cells lying at the same side of the sieve tube element in the 'Fridericia and allies clade' (except from *Lundia*), *Pleonotoma* and *Stizophyllum* (Fig. 7D), but a single origin of two companion cells lying at the two opposing sides of the sieve element in *Adenocalymma*, although the ancestor of *Adenocalymma* was reconstructed as having a single companion cell lying on the corner of the sieve tube (Fig. 7D).

Axial phloem parenchyma Axial parenchyma generally occupies <50 % of the transverse area (Table 1). Short radial rows of three to seven cells are ubiquitous in the variant phloem, intersecting other cell types. In addition to these radial rows, two types of arrangements were delimited: (1) diffuse (Fig. 8A) and (2) sieve-tubecentric (Fig. 8B). Sieve-tubecentric axial
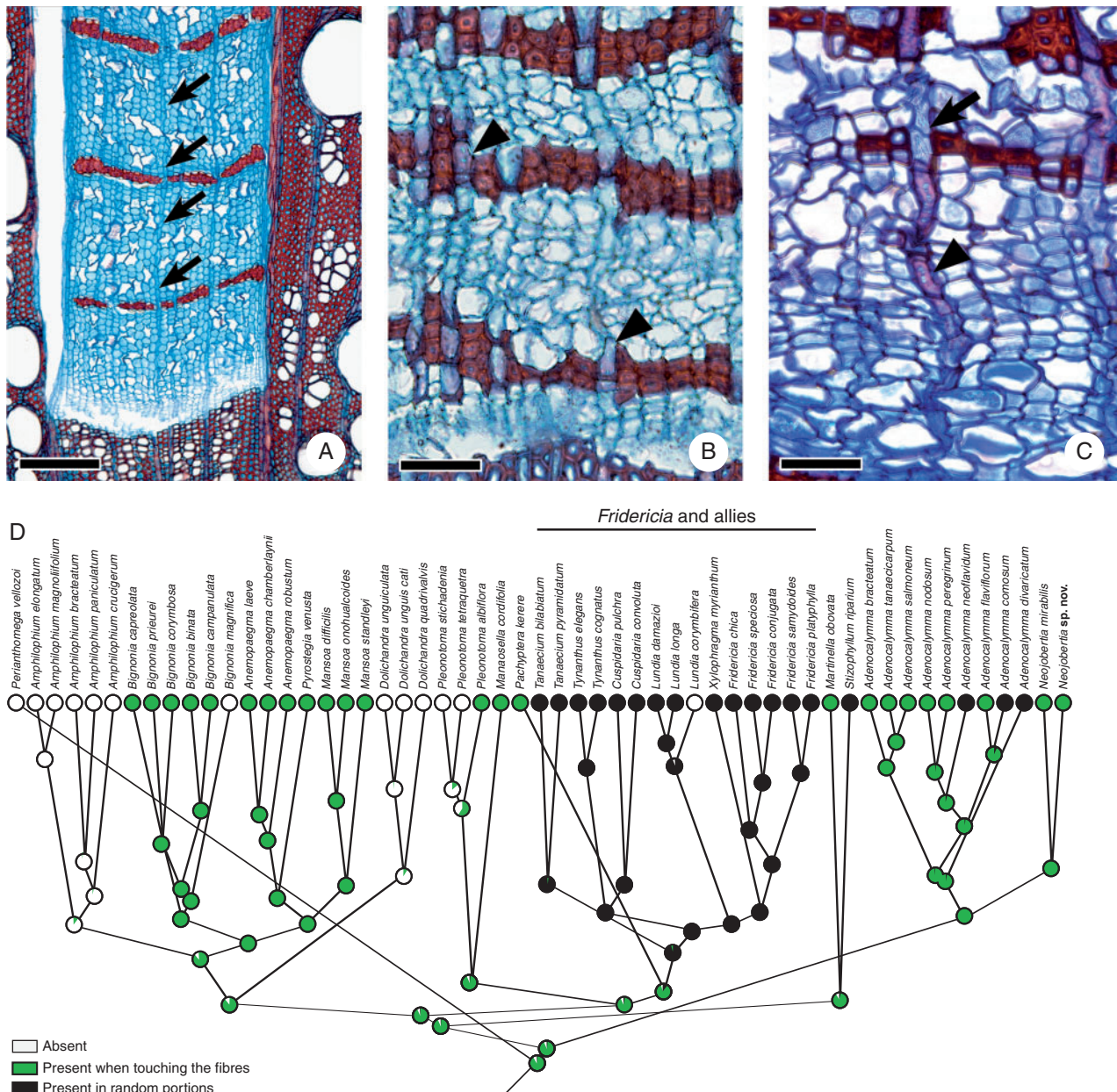
FIG. 9. Ray lignification on the variant phloem. (A) Transverse section of *Amphilophium crucigerum*. Rays are never lignified (arrows). (B) Transverse section of *Adenocalymma peregrinum*. Rays lignify only when touching the fibre bands (arrowheads). (C) Transverse section of *Tanaecium pyramidatum*. Rays are lignified (arrowhead) or non-lignified (arrow), randomly distributed. (D) Ancestral character state reconstruction of ray lignification. Scale bars (A) = 200 μm; (B, C) = 50 μm.

parenchyma forms a sheath of cells around each sieve tube element (Fig. 8B).

Ancestral character state reconstruction revealed that the ancestral state for the tribe was the diffuse axial parenchyma type (Fig. 8C), with multiple independent origins of the sieve-tubecentric: once in *Pleonotoma*, once in the '*Fridericia* and allies clade', once in *Neojobertia* and probably more than once in *Adenocalymma* (Fig. 8C).

When the axial parenchyma of the variant phloem was analysed for directional evolution, we encountered no directionality (Table 2). Furthermore, tree-scaling parameters indicated that the axial parenchyma evolved independently of branch lengths (gradually, $\kappa = 1 \cdot 1$) and independently of phylogeny

($\lambda = 0 \cdot 28$), accelerating towards the terminals (species-specific adaptation; $\delta = 3$).

Lignification of the phloem rays Rays are predominantly uniseriate to biseriate in the variant phloem (Figs 4B and 9), except for the limiting rays. The diversity of rays is related to their state of lignification. Three different states of lignification are encountered: (1) non-lignified, where the rays are never lignified, not even when crossing the fibre bands (Fig. 9A); (2) rays always lignified when crossing the fibre bands (Fig. 9B); and (3) rays randomly lignified, sometimes lignified when touching the fibre bands and sometimes lignified far from them (Fig. 9C).
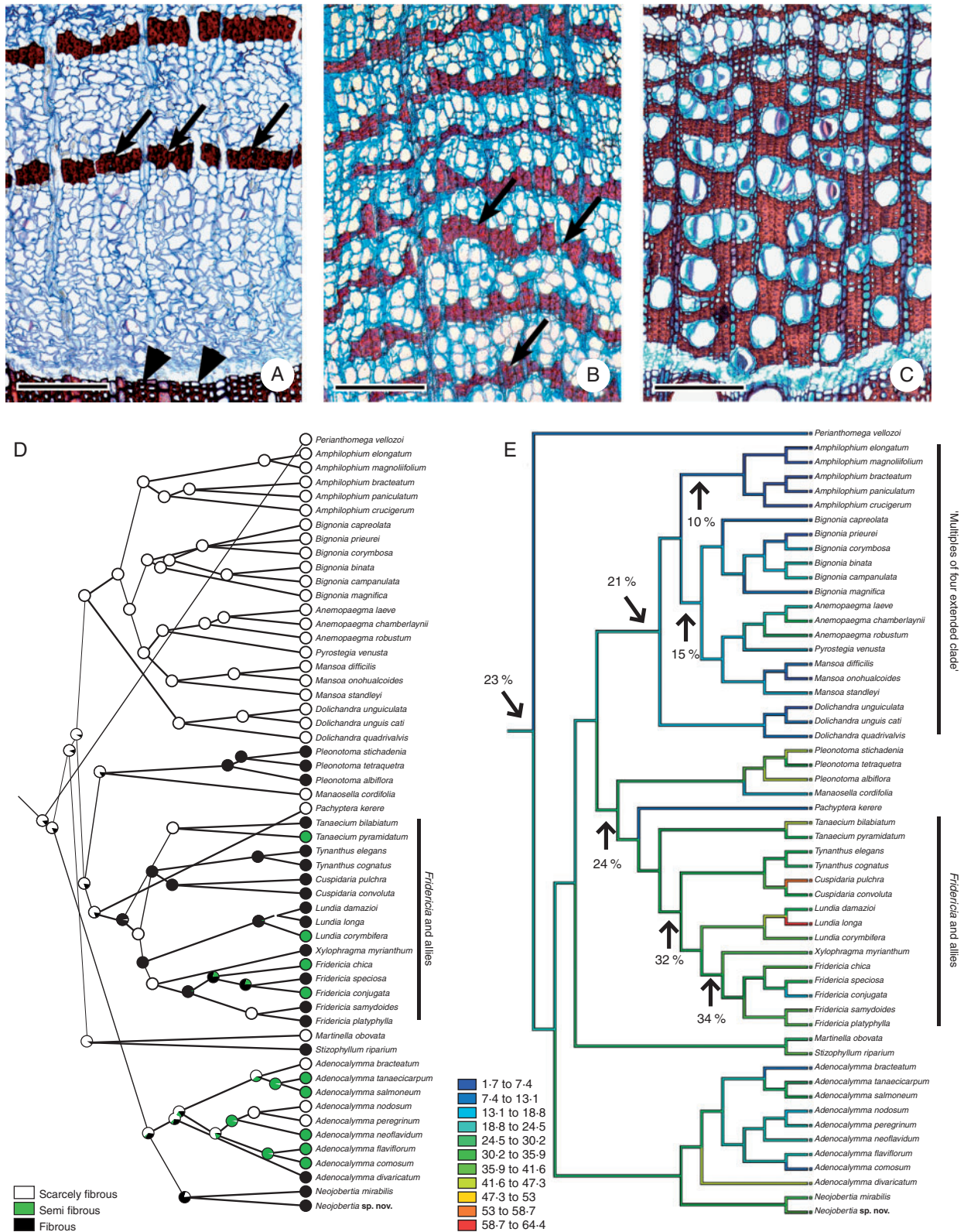
FIG. 10. Phloem types according to their fibre arrangement in variant phloem. (A) Transverse section of *Callichlamys latifolia*, a scarcely fibrous species, with more than ten cells of phloem parenchyma and sieve tube elements between fibre bands (arrows). Note that the phloem fibres (arrows) are thicker than the xylem fibres (arrowheads). (B) Transverse section of *Adenocalymma comosum*, a semifibrous species, with fewer than ten cells of phloem parenchyma and sieve tube elements between fibre bands (arrows). Note the undulated arrangement of the fibre bands. (C) Transverse section of *Xylophragma myrianthum*, a fibrous species, with the fibres forming a background tissue where other cell types are embedded. (D) Ancestral character state reconstruction of phloem type evolution. (E) Ancestral character state reconstruction of the percentage of fibres per tranverse area. Scale bars (A, B) = 200 μm; (C) = 120 μm.

Fig. 11. Storied elements in the variant phloem. (A) Longitudinal tangential section of *Callichlamys latifolia*, without a storied structure. (B) Longitudinal tangential section of *Amphilophium elongatum*, with axial elements stori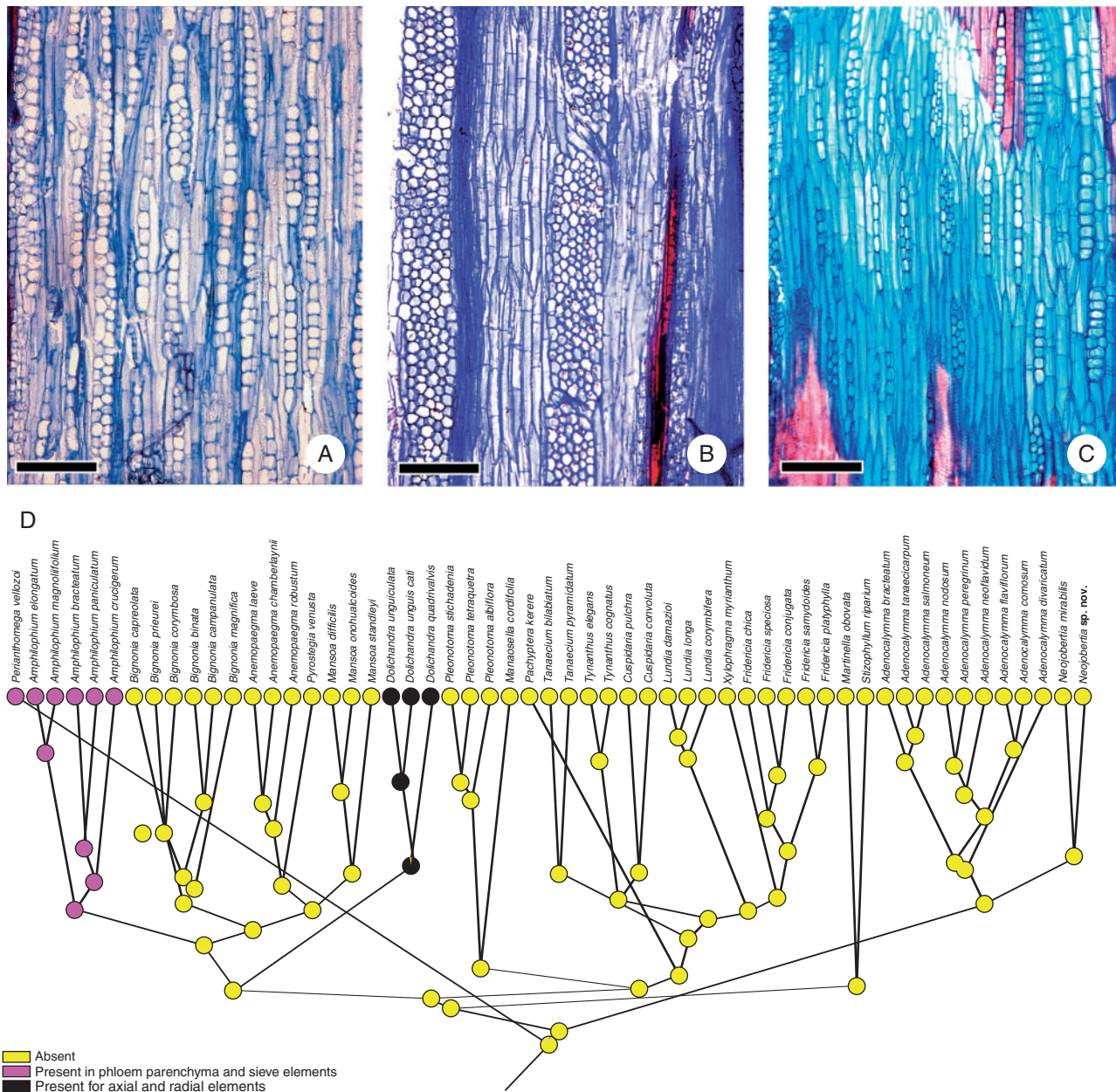ed. (C) Longitudinal tangential section of *Dolichandra unguis-cati*, with radial and axial elements storied. (D) Ancestral state reconstruction of the storied structure evolution. Scale bars = 200 μm.

Ancestral character state reconstruction revealed that the ancestral state for the tribe was having rays that lignify only when touching the fibre bands (Fig. 9D). Six independent origins of rays that never lignify have occurred: once in *Perianthomega*, once in *Amphilophium*, once in *Bignonia magnifica*, once in *Dolichandra*, once in *Pleonotoma* (except *P. albiflora*) and once in *Lundia corymbifera*. The ancestral state for both *Bignonia* and *Lundia* was having rays that lignify when touching the fibre bands (Fig. 9D). The 'Fridericia and allies clade' is marked by the exclusive presence of rays that lignify in random portions, except for a reversal in *Lundia corymbifera* (Fig. 9D).

Fibre Phloem fibres are generally more thick-walled than xylem fibres, as seen in transverse section (Fig. 10A, C). Depending on the abundance of fibres, it is possible to qualitatively divide the variant phloem into three types: (1) scarcely fibrous; (2) semifibrous; and (3) fibrous. Scarcely fibrous phloem is marked by the presence of fibre bands two to five cells wide that alternate with more than ten cells of phloem parenchyma and sieve tube elements (Fig. 10A). Semifibrous phloem has undulated fibre bands that alternate with fewer than ten cells of sieve elements and phloem parenchyma between them (Fig. 10B). Finally, fibrous phloem has fibres that are closely arranged, forming a background tissue in which all other cells are embedded (Fig. 10C).
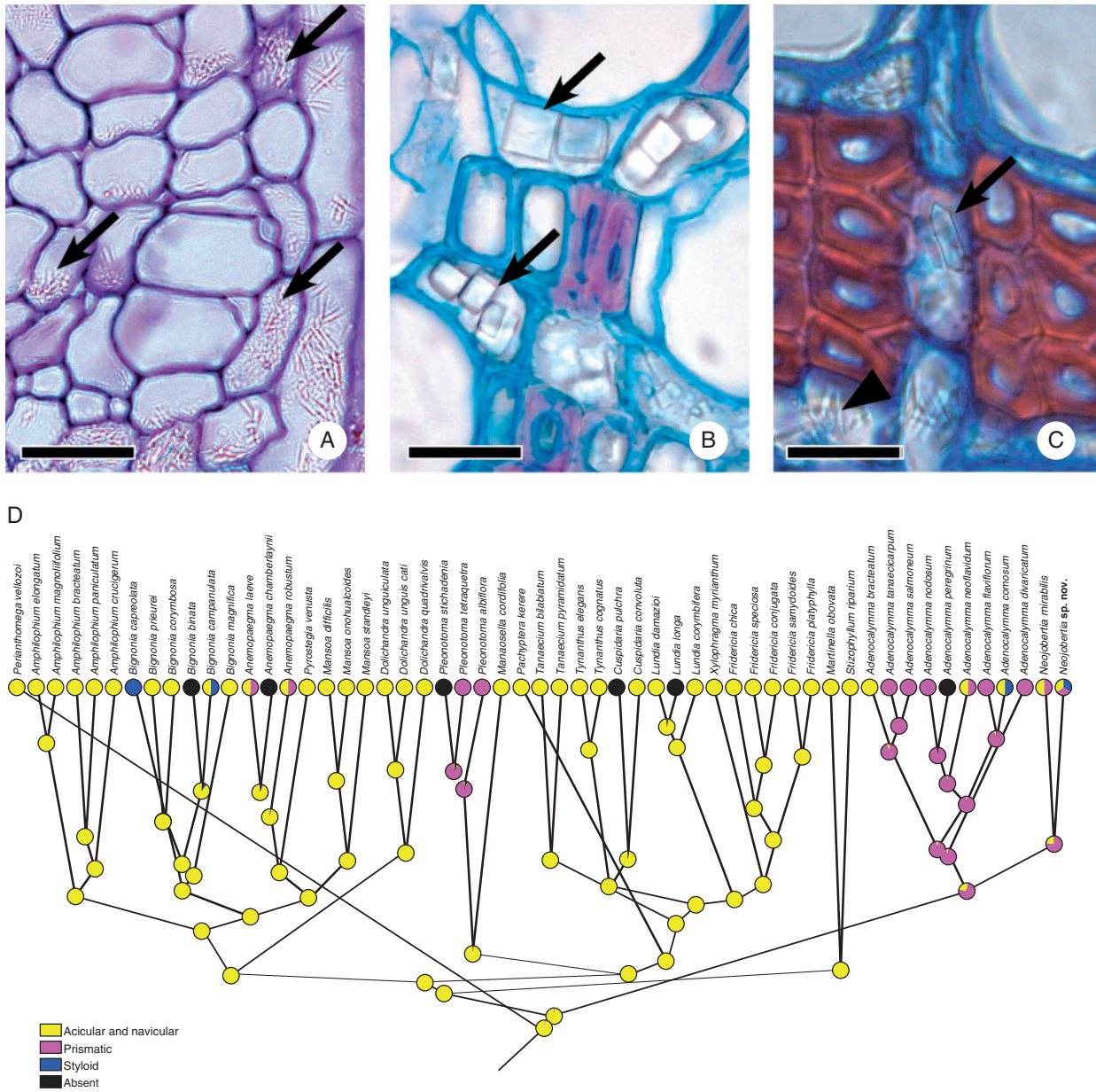
FIG. 12. Crystal types in the phloem and ray parenchyma. (A) Transverse section of *Perianthomega vellozoi*: acicular crystals (arrows). (B) Transverse section of *Pleonotoma tetraquetra*: prismatic crystals (arrows). (C) Transverse section of *Neojobertia* sp. nov.: elongate crystal (arrow) and acicular crystals (arrowhead). (D) Ancestral character state reconstruction of crystal type in the phloem and ray parenchyma. Scale bars (A, B) = 30 μm; (C) = 20 μm.

Ancestral state reconstruction of fibre band types revealed that the ancestral state for the tribe was the scarcely fibrous type, with well-spaced fibre bands (stratified phloem), and multiple parallel origins of the two other types (Fig. 10D). The entire 'Fridericia and allies clade', *Stizophyllum*, *Neojobertia* and *Pleonotoma* have fibrous phloems.

When the percentage of fibres per total phloem area (Table 1) was mapped as a continuous character (Fig. 10E), followed by directional analysis (Table 2), it was seen that the tribe as a whole exhibited no sign of directional evolution. However, when certain lineages were considered separately within the tribe, two contrasting results were found. Some lineages exhibited directional evolution towards a decrease in the amount of fibres (Table 2; Fig. 10E), such as the 'Multiples of

four extended clade', while other lineages exhibited directional evolution towards an increase in fibre abundance, such as the 'Fridericia and allies extended clade' (Table 2). Fibres in the tribe as a whole seems to be evolving toward higher stasis in the long branches (Table 2), in a more punctuated fashion ($\kappa = 0.27$), with closely related taxa resembling each other ($\lambda = 0.81$), within a mode compatible with Brownian motion (default gradualism; $\delta = 1.33$).

When the two major lineages of the tribe were analysed for parameters of evolution, contrasting models were demonstrated again. In the 'Fridericia and allies extended clade', the parameter showed that this lineage differed from the tribe in having minimal effect of phylogeny ($\lambda = 0.33$) and accumulating changes in the long branches (species-specific adaptation;
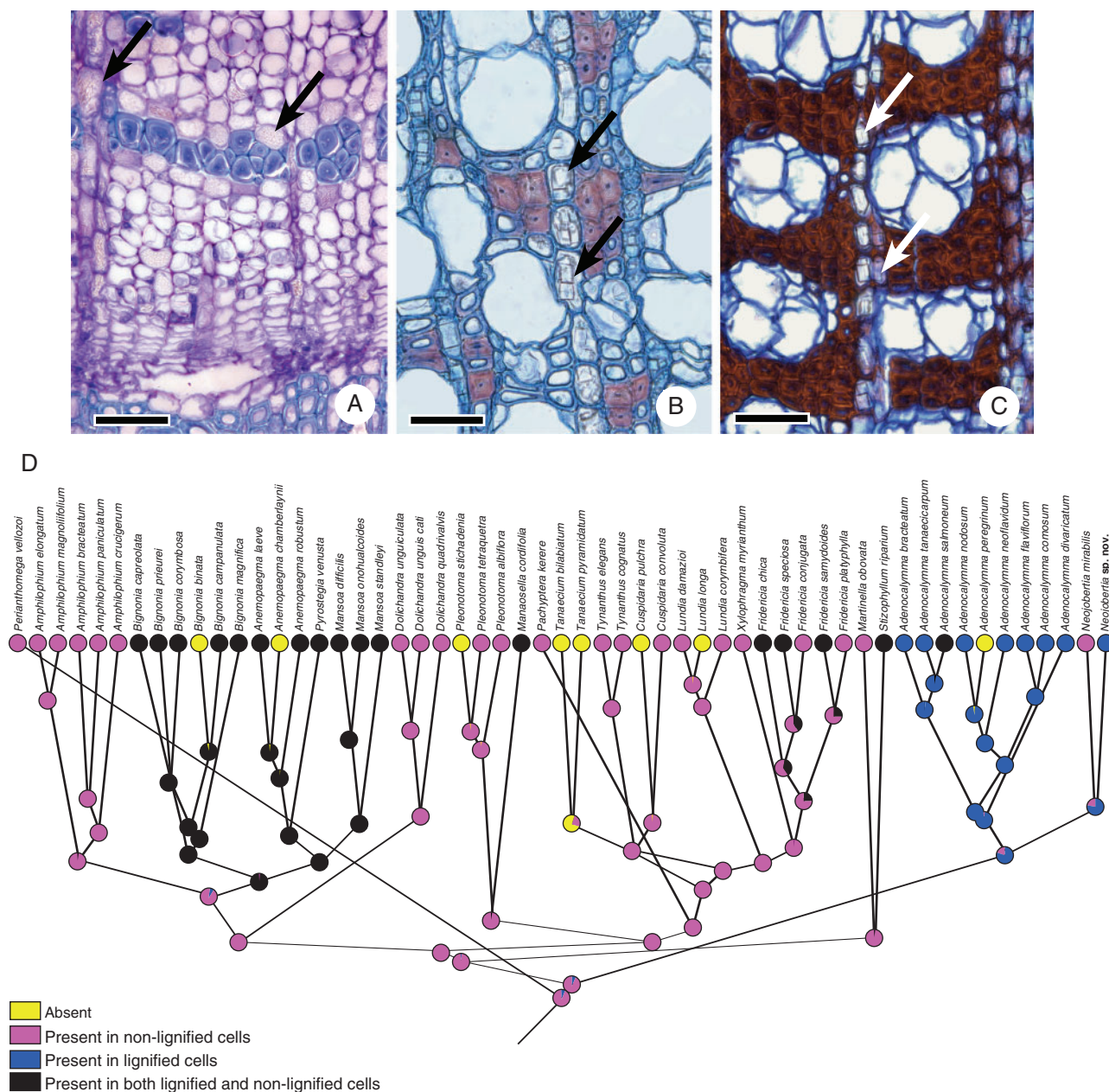
FIG. 13. Location of crystals according to the lignification state of the parenchyma cells. (A) Transverse section of *Bignonia magnifica*. Acicular crystals are present in non-lignified axial and ray parenchyma cells. (B) Transverse section of *Pleonotoma tetraquetra*. Prismatic crystals are present in the non-lignified ray cells. (C) Transverse section of *Adenocalymma divaricatum*. Prismatic crystals are present in lignified ray cells. (D) Ancestral character state reconstruction of the presence and place of occurrence of the crystals. Scale bars (A–C) = 50 μm.

$\delta = 2 \cdot 8$). The 'Multiples of four extended clade' differed only in the fact that most changes occurred early in the phylogeny, followed by stasis, a scenario compatible with adaptive radiation ($\delta = 0 \cdot 68$).

Storied structure A storied structure is absent in most genera (Fig. 11A), being present exclusively in *Amphilophium*, *Dolichandra* and *Perianthomega* (Fig. 11B–D). In both *Amphilophium* and *Perianthomega*, only the axial elements are storied (parenchyma, sieve tube elements and fibres; Fig. 11B), while in *Dolichandra* both axial and radial elements are storied (Fig. 11C).

Ancestral character state reconstruction showed that the ancestral state in the tribe was unambiguously a non-storied structure (Fig. 11D), with three independent origins of a storied structure: once in *Amphilophium*, once in *Perianthomega* and once in *Dolichandra* (Fig. 11D).

Crystal inclusions in the secondary phloem

The presence of crystals is widespread in Bignonieae. However, their type and location are variable. Three distinct types of crystals are found in the axial and ray parenchyma: (1)
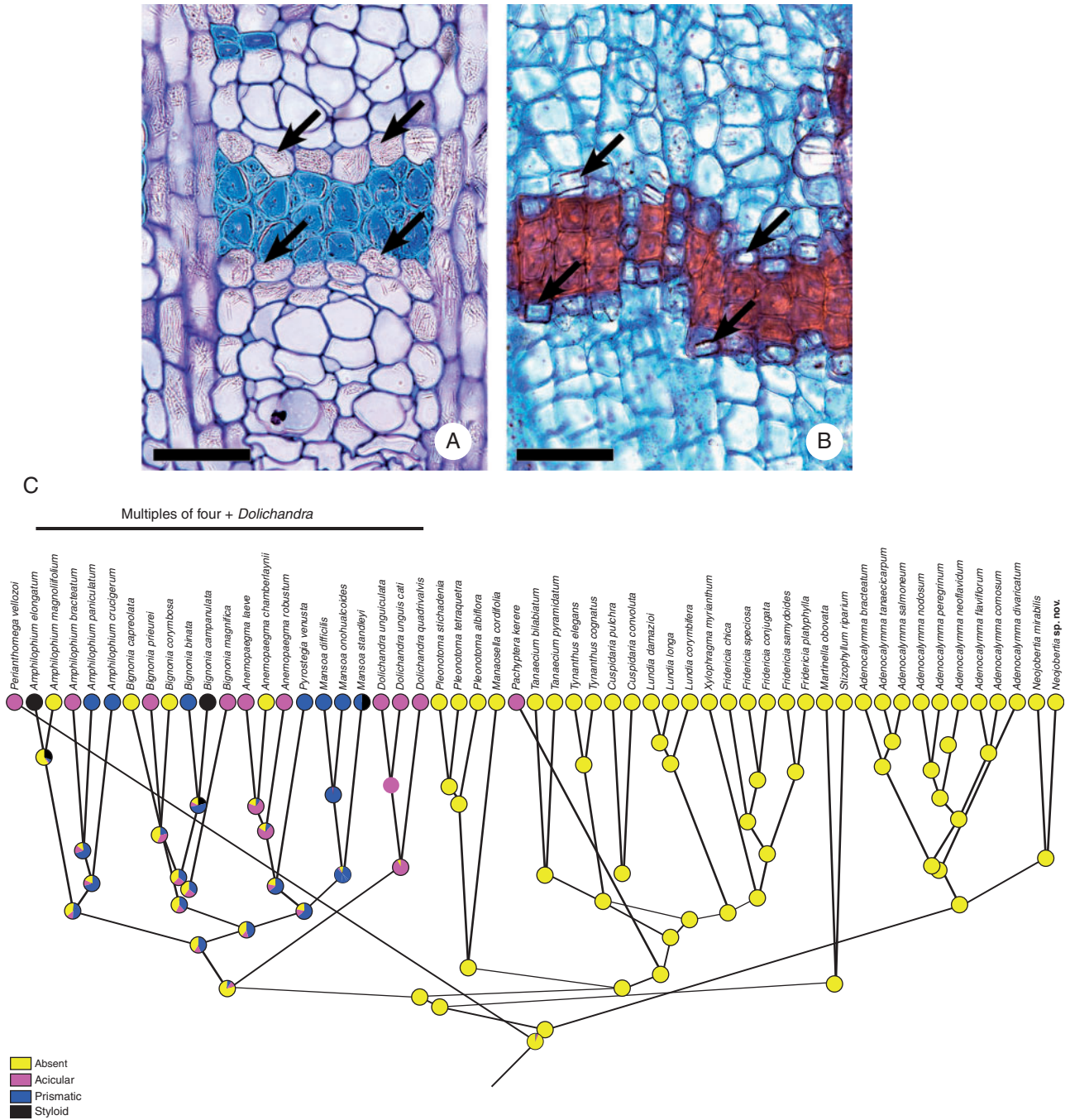
FIG. 14. Types of crystal in fibre-associated crystalliferous parenchyma. (A) Transverse section of *Perianthomega vellozoi* crystalliferous parenchyma sheath bearing acicular crystals (arrows). (B) Transverse section of *Mansoa standley*: crystalliferous parenchyma sheath bearing prismatic crystals (arrows). (C) Ancestral character state reconstruction of type of crystals in fibre-associated crystalliferous parenchyma. Scale bar = 50 μm.

acicular (Fig. 12A), (2) prismatic (Fig. 12B) and (3) styloid/elongate (Fig. 12C).

Ancestral character state reconstruction revealed that the ancestral state for the tribe was the presence of acicular crystals (Fig. 12D), with two to four independent origins of phloem and ray parenchyma bearing prismatic crystals, once in the clade formed by *Adenocalymma* and *Neojobertia* and another in *Pleonotoma* (Fig. 12D). Two *Adenocalymma* species (*A. laeve* and *A. robustum*) are polymorphic, with prismatic and acicular crystals co-occurring (Fig. 12D). Styloid and elongate crystals are found exclusively in four of the analysed species: *Adenocalymma comosum*, *Neojobertia* sp. nov., *Bignonia campanulata* and *Bignonia capreolata*. However, except for *B. capreolata*, the other species are polymorphic, always having

Overall phloem anatomy   **Morphology of sieve elements**   **Storied structure**

Scarcely to semi-fibrous Stratified phloem

Fibrous Non-stratified phloem
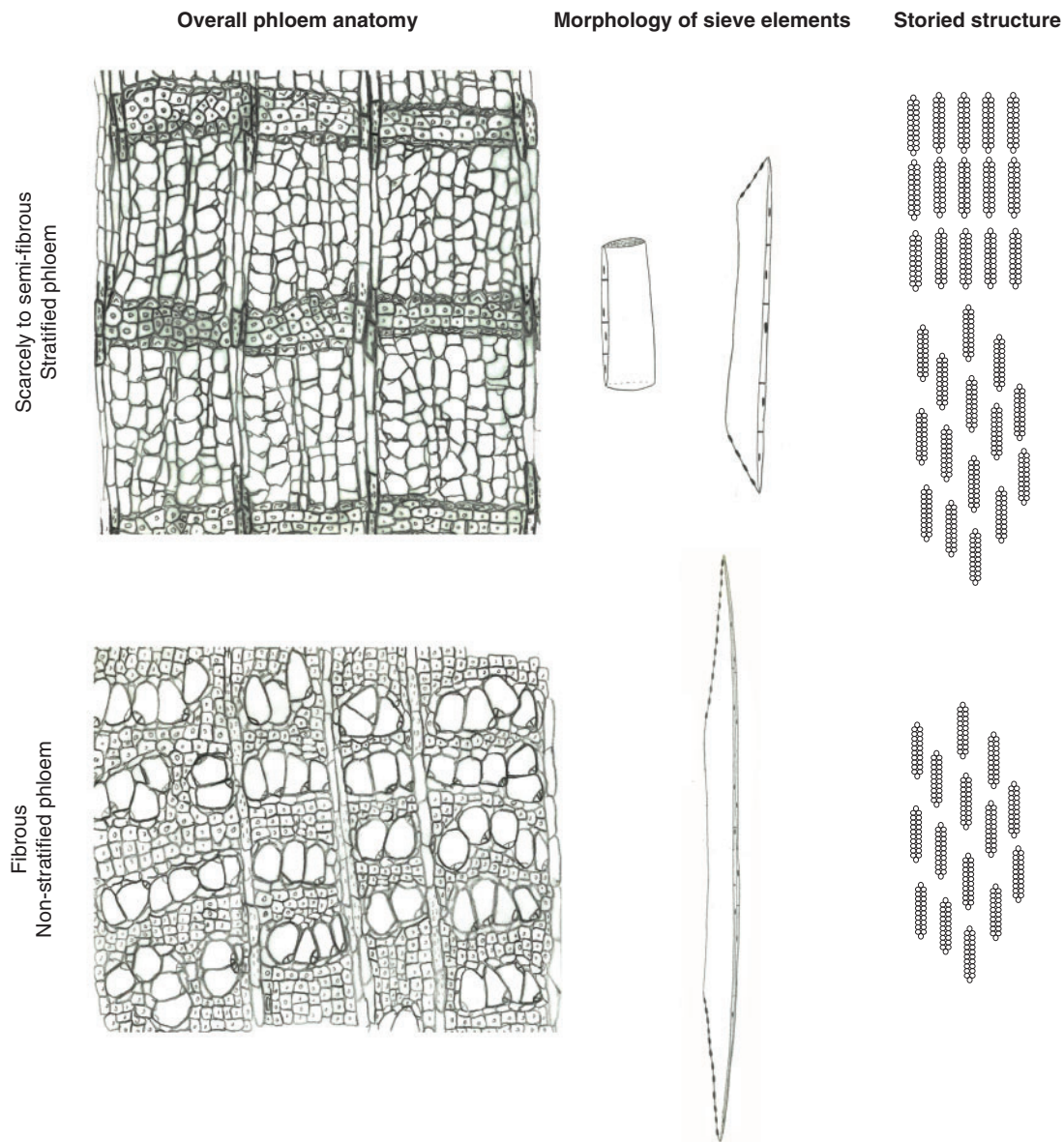
F‍IG. 15. Drawing summarizing the two contrasting phloem anatomies present in Bignonieae (Bignoniaceae).

acicular crystals mixed with the styloid/elongate crystals, and co-occurring with prismatic crystals in the case of *Neojobertia* sp. nov. (Fig. 12C).

Crystals are found exclusively in the non-lignified axial and ray parenchyma cells (Fig. 13A, B), exclusively in lignified cells (Fig. 13C), and in both lignified and non-lignified cells. Only rarely are crystals absent altogether.

Ancestral state reconstructions indicated that the ancestor of all Bignonieae likely had crystals in the non-lignified parenchyma (Fig. 13D) and further suggest a single origin in *Adenocalymma* for species with crystals exclusively in the lignified cells (Fig. 13D) and at least five independent origins for the presence of crystals in both lignified and non-lignified axial and ray parenchyma, as observed in the 'Multiples of four

clade', except *Amphilophium*, in *Manaosella cordifolia*, in *Fridericia* and in *Adenocalymma* (Fig. 13D).

In species with scarcely fibrous and semifibrous phloem, parenchyma sheaths bearing crystals are common around the fibre bands (Fig. 14A, B). Ancestral state reconstruction revealed unequivocally that the ancestral state for the tribe is the absence of crystalliferous sheaths (Fig. 14C). Three lineages, however, have such crystalliferous sheaths, *Perianthomega*, *Pachyptera* and the members of the 'Multiple of four' extended clade, except for punctual reversals (Fig. 14D), such as that of *Amphilophium magnoliifolium*, *Bignonia capreolata*, *B. corymbosa* and *Anemopaegma chamberlaynii*. A single origin for the appearance of prismatic crystals was inferred for the 'Multiples of four clade' and

TABLE 1. *Anatomical characters of the variant phloem of Bignonieae (Bignoniaceae)*

Taxon	Lateral steps on the phloem wedges[1]	Limiting ray lignification[2]	Storied structure[3]	Sieve tube arrangement[4]	Sieve plate type[5]	Sieve areas per sieve plate (average)	Number of companion cells[6]	Percentage of parenchyma per transverse area	Phloem parenchyma type[7]	Ray lignification[8]	Phloem type according to fibre frequency[9]	Percentage of fibres	Crystals in phloem and ray parenchyma[10]	Type of crystals in phloem and ray parenchyma[11]	Crystalliferous parenchyma sheath	Type of crystal in the crystalliferous parenchyma sheath[11]
Adenocalymma bracteatum	A	X	—	R	C	7	1	?	D	+F	SCF	10·8	L	A	—	—
Adenocalymma comosum	A	X	—	T	C	14	1	29·7	D	+R	SCF	11·7	L	A/S	—	—
Adenocalymma divaricatum	A	X	—	T	C	8	—	10·6	STC	+R	F	46·6	L	P	—	—
Adenocalymma flaviflorum	A	X	—	R	C	8	2D	32·2	D	+F	F	23·3	L	P	—	—
Adenocalymma neoflavidum	A	X	—	T	C	6	2D	20·9	STC	+R	SF	23·8	L	A/P	—	—
Adenocalymma nodosum	A	na	—	R	C	7	2D	42·1	D	+F	SCF	15·9	L	P	—	—
Adenocalymma peregrinum	A	X	—	R	C	6	2D	32·3	D	+F	SF	19·4	L	—	—	—
Adenocalymma salmoneum	A	XP	—	T	C	7	—	21·2	STC	+R	SF	32·5	L/N	P	—	—
Adenocalymma tanaecicarpum	A	X	—	C	6	1	?	D	+F	SF	30·1	L	P	—	+	?
Amphilophium bracteatum	A	X	A	D	S	1	1	?	D	—	SCF	2·1	N	A	+	P
Amphilophium crucigerum	A	X	A	D	S	0	1	66·3	D	—	SCF	3·6	N	A	+	S
Amphilophium elongatum	A	X	A	D	S	1	1	17·2	D	—	SCF	1·9	N	A	+	?
Amphilophium magnoliifolium	A	X	—	D	S	2	1	?	D	—	SCF	1·7	N	A	+	P
Amphilophium paniculatum	A	X	A	D	S	0	1	25·2	D	—	SCF	2·0	N	A	—	—
Anemopaegma chamberlaynii	A	X	A	R	C	5	1	29·9	D	+F	SF	31·8	—	—	—	A
Anemopaegma laeve	A	X	—	R	C	4	1	25·4	D	+F	SCF	20·8	B	A/P	+	A
Anemopaegma robustum	A	X	—	R	C	5	1	28·3	D	+F	SCF	28·2	B	A/P	+	P
Bignonia binata	A	X	—	R	C	10	1	26·5	D	+F	SCF	19·9	—	—	+	S
Bignonia campanulata	A	X	—	R	C	8	1	22·5	D	+F	SCF	20·0	B	A/S	+	—
Bignonia capreolata	A	X	—	R	C	5	1	?	D	+F	SCF	12·0	B	S	—	—
Bignonia corymbosa	A	X	—	R	C	?	1	?	D	?	SCF	15·0	?	?	+	?
Bignonia magnifica	A	X	—	R	C	7	1	43	D	—	SCF	10·0	B	A	+	A
Bignonia prieurei	A	X	XP	R	C	?	1	?	D	?	SCF	6·0	B	A	+	?
Cuspidaria convoluta	S	XP	—	T	C	26	2S	18·0	STC	+R	SF	32·1	N	A	—	—
Cuspidaria pulchra	S	XP	—	T	C	17	2S	16·7	STC	+R	SF	55·2	N	A	—	—
Dolichandra quadrivalvis	A	—	AR	R	C	4	1	31	D	—	SCF	10·0	N	A	+	A
Dolichandra unguiculata	A	—	AR	R	C	4	1	29·3	D	—	SCF	6·4	N	A	+	A
Dolichandra unguis-cati	A	—	AR	R	C	6	1	40·1	D	+R	SCF	11·4	N	A	+	A
Fridericia chica	A	XP	—	T	C	18	2S	25·9	STC	+R	SF	36·2	B	A	—	—
Fridericia conjugata	A	XP	—	T	C	15	2S	35·3	STC	+R	SF	17·3	N	A	—	—
Fridericia platyphylla	A	XP	—	T	C	14	2S	16·8	STC	+R	F	38·7	B	A	—	—
Fridericia samydoides	A	XP	—	T	C	26	2S	23·4	STC	+R	F	36·3	B	A	—	—
Fridericia speciosa	A	XP	—	T	C	18	2S	19·0	STC	—	SF	32·8	B	A	—	—
Lundia corymbifera	A	X	—	T	C	16	1	31·4	STC	+R	SF	36·0	B	A	—	—
Lundia damazioi	A	X	—	T	C	18	1	18·9	STC	+R	SF	32·6	?	A	—	—
Lundia longa	A	X	—	T	C	15	1	11·6	STC	+R	F	58·7	N	—	—	—
Manaosella cordifolia	S	X	—	D	C	12	1	30·6	D	+F	SCF	14·7	—	A	—	—
Mansoa difficilis	A	X	—	R	C	5	1	37·4	D	+F	SCF	8·1	B	A	—	—
Mansoa onohualcoides	A	X	—	R	C	5	1	?	D	+F	SCF	7·0	B	A	+	P
Mansoa standleyi	A	X	—	R	C	9	1	36·1	D	+F	SCF	18·2	B	A	+	P/S
Martinella obovata	?	XP	—	R	C	?	1	30·5	D	+F	SF	30·0	?	?	—	—
Neojobertia mirabilis	A	X	—	T	C	8	1	21·5	STC	+F	F	40·1	L	A/P	—	—
Neojobertia sp. nov.	A	X	—	T	C	10	1	18·8	STC	+F	F	39·4	N	A/S/P	—	—
Pachyptera kerere	A	X	—	R	C	7	1	37·4	D	+F	SCF	13·0	N	A	—	A
Perianthomega vellozoi	A	X	—	R	S	0	1/2D	37·4	D	—	SCF	8·4	N	A	+	A
Pleonotoma albiflora	A	XP	—	T	C	40	2S	?	STC	+	F	44·2	N	P	+	—
Pleonotoma stichadenia	A	x	—	T	C	34	2S	22·2	STC	—	SF	45·8	?	?	—	?

(continued)

TABLE 1. *Continued*

| Taxon | Secondary phloem characters and character states | | | | | | | | | | | | | | Cell inclusions in the phloem | | |
	Lateral steps on the phloem wedges[1]	Limiting ray lignification[2]	Storied structure[3]	Sieve tube arrangement[4]	Sieve plate type[5]	Sieve areas per sieve plate (average)	Number of companion cells[6]	Percentage of parenchyma per transverse area	Phloem parenchyma type[7]	Ray lignification[8]	Phloem type according to fibre frequency[9]	Percentage of fibres	Crystals in phloem and ray parenchyma[10]	Type of crystals in phloem and ray parenchyma[11]	Crystalliferous parenchyma sheath	Type of crystal in the crystalliferous parenchyma sheath[11]
Pleonotoma tetraquetra	A	X	–	T	C	37	2S	32·5	STC	–	SF	34·8	N	P	–	–
Pyrostegia venusta	A	X	–	R	C	6	1	37·6	D	+F	SCF	15·3	B	A	+	P
Stizophyllum riparium	A	XP	–	T	C	8	2S	11·9	STC	+R	F	36·9	B	A	–	–
Tanaecium bilabiatum	na	XP	–	T	C	17	2S	21·0	STC	+R	F	44·7	–	?	–	–
Tanaecium pyramidatum	na	XP	–	T	C	19	2S	28·4	STC	+R	SF	35·6	N	?	–	–
Tynanthus cognatus	S	XP	–	T	C	19	2S	22·6	STC	+R	F	26·6	N	A	–	–
Tynanthus elegans	S	XP	–	T	C	21	2S	20·6	STC	+R	F	35·1	N	A	–	–
Xylophragma myrianthum	A	XP	–	T	C	25	2S	16·4	STC	+R	F	41·0	N	A	–	–

For continuous variables, 'Number' represents the mean of an overall sample of 30.
+, present; −, absent; ?, not sampled; na, not applicable.
[1]A, asymmetrical; S, symmetrical. [2]X, to the xylem face; XP, to both faces. [3]A, present in axial parenchyma; AR, present in axial and ray parenchyma. [4]R, radial; T, tangential; D, diffuse. [5]S, mostly simple; C, compound. [6]1, one per sieve tube; 2D, two per sieve tube at different sides; 2S, two or more per sieve element at the same side. [7]STC, sieve-tubecentric; D, diffuse. [8]+R, present in random portions; +F, present when touching the fibre bands. [9]SCF, scarcely fibrous; SF, semi-fibrous; F, fibrous. **Fibres:** N, narrow; W, wide. [10]L, present in lignified cells; N, present in non-lignified cells; B, present in both lignified and non-lignified cells. [11]A, acicular; P, prismatic; S, styloid or elongate.

multiple origins for both the acicular crystals and the styloid/elongate crystals within the crystalliferous parenchyma (Fig. 14C).

Correlation analyses

In the literature, some characters were hypothesized to evolve in correlation (see Introduction). Here we tested the correlations between (1) sieve tube length and sieve plate type, and (2) sieve tube length and storied structure. Also, we tested several characters in relation to fibre abundance, such as (1) sieve plate type, (2) sieve tube arrangement, (3) parenchyma type, (4) ray lignification and (5) two or three companion cells lying at the same side of the sieve tube. The results from correlation analyses are summarized in Table 3.

Sieve tube length showed positive correlation with both sieve plate type and storied structure ($P < 0.01$; LRTs 13·44 and 27·17, respectively). Therefore, short sieve tubes usually bear simple sieve plates, while long sieve tubes bear compound sieve plates. Whenever a storied structure is present the sieve tubes are short.

Regarding fibre abundance, we encountered a positive correlation with sieve plate type, sieve tube arrangement, parenchyma type and number of companion cells ($P < 0.01$, LRTs 25·00, 25·01, 17·54 and 8·72, respectively), indicating that the sieve tubes have a compound sieve plate, tangential arrangement of the sieve tubes, sieve-tubecentric phloem parenchyma and two or three companion cells lying at the same side of the sieve tube whenever the phloem has a higher abundance of fibres. Correlation between lignification of rays and fibre abundance was rejected ($P = 0.79$; LRT 0·66).

DISCUSSION

Growth dynamic of the phloem wedges

Stems of Bignonieae have a very particular growth dynamic. At the onset of development, the stem has the exact same pattern of growth as that of most woody plants, with the vascular cambium producing more xylem to the inside and less phloem to the outside and with equal activity across its entire girth (Dobbins, 1969; Pace *et al.*, 2009). Soon in development, however, four equidistant portions of the cambium switch from a regular to a variant activity, with these variant cambia ceasing to divide anticlinally and starting to produce less secondary xylem and more secondary phloem, eventually producing deep phloem wedges that furrow the xylem (Dobbins, 1971; Pace *et al.*, 2009, 2015). Because the variant cambia do not divide anticlinally and remain at the same limited size, while all the tissues around them progress normally the secondary growth, these four variant portions must accommodate their growth in order to keep up with the stem thickening without risking the occurrence of ruptures. In Bignonieae, this occurs by means of two different mechanisms: production of tall multiseriate limiting rays and lateral phloem steps.

Ray enlargement to accommodate secondary growth has long been known to occur in the secondary phloem, being extremely conspicuous in e.g. the Malvaceae *s.l.* (Metcalfe and Chalk, 1950). However, these limiting rays, term coined by Schenck (1893), are not all equal and vary in their lignification

TABLE 2. *Scaling parameters of evolution for the continuous characters analysed following* Pagel (1999), *and their implications for the pattern of evolution of these characters*

Character	κ	Branch length scale	λ	Contribution of phylogeny	δ	Total path scale	Model A	Model B	LR
Sieve-tube areas	0·0*	Punctuational evolution	0·0*	Star phylogeny (species-independent)	3·0*	Temporally later change (species-specific adaptation)	−225·65	−226·22	−1·14
Variant parenchyma (%)	1·1	Default gradualism	0·28*	Minimal effect of phylogeny	3·0*	Temporally later change (species-specific adaptation)	−176·79	−177·66	−1·75
Fibres in variant phloem of the entire tribe (%)	0·27*	Stasis in longer branches	0·81	Default phylogeny	1·33	Default gradualism	−207·64	−208·03	−0·78
Fibres in variant phloem of 'Fridericia and allies extended clade' (%)	0·44*	Stasis in longer branches	0·33*	Minimal effect of phylogeny	2·8*	Temporally later change (species-specific adaptation)	−77·28	−87·30	−20·04
Fibres in variant phloem of 'Multiples of four extended clade (%)	0·16*	Stasis in longer branches	0·99	Default phylogeny	0·68*	Adaptive radiation	−69·35	−70·43	−2·17
Number of sieve areas in variant phloem of 'Fridericia and allies extended clade'	2·28*	Longer branches accumulate more changes	1·0	Default phylogeny	0·30*	Adaptive radiation	−60·74	−60·77	−0·06
Number of sieve areas in variant phloem of 'Multiples of four extended clade	0·0*	Punctuational evolution	0·94	Default phylogeny	0·54*	Adaptive radiation	−46·75	−54·15	−14·80

*Significant deviations from 1·0 for the scaling parameters values kappa (κ), lambda (λ), and delta (δ), assessed with the likelihood ratio (LR) test.
LR values greater than 2 indicate directional evolution.

TABLE 3. Pagel's 1994 *correlation analyses of discrete phloem characters, from 1000 simulations. Continuous characters were made categorical and their respective character states are presented in parentheses*

	Log likelihood under four-parameter model	Log likelihood under eight-parameter model	Difference between log likelihoods	*P* value
Length of sieve tube (shorter or longer than 500 μm) and sieve plate type (simple or compound)	−38·86	−25·41	13·44*	<0·01*
Length of sieve tube (shorter or longer than 500 μm) × storied structure (absent or present)	−36·18	−9·01	27·17*	<0·01*
Percentage of fibres (non-fibrous or semi-fibrous to fibrous) × compound sieve plates (absent or present)	−52·81	−27·80	25·00*	<0·01*
Percentage of fibres (non-fibrous or semi-fibrous to fibrous) × tangential arrangement of sieve tubes (absent or present)	−58·27	−33·26	25·01*	<0·01*
Percentage of fibres (non-fibrous or semi-fibrous to fibrous) × sieve-tubecentric parenchyma (absent or present)	−45·23	−27·69	17·54*	<0·01*
Percentage of fibres (non-fibrous or semi-fibrous to fibrous) × ray lignification (absent or present)	−43·59	−42·92	0·66	0·798
Percentage of fibres (non-fibrous or semi-fibrous to fibrous) × 2 or 3 companion cells on the same side (absent or present)	−38·34	−29·62	8·72*	<0·01*

*Significant correlations.

state. The limiting rays may be entirely non-lignified, only lignified next to the xylem face, or lignified at both sides but with a core middle part of non-lignified ray cells. Given that the variant cambia are included within the phloem wedges and surrounded by a matrix of stiff secondary xylem, a non-lignified ray portion, even if just a central core, is critical to allow cell division in order to guarantee the possibility of cell dislocation from within the wedges. Thus, while cambial derivatives are periodically formed and pushed outwards from within the phloem wedges, the limiting rays divide along with these newly formed phloem cells. This mechanism was first proposed for

African Hippocrateoideae (Celastraceae *s.l.*), which also have disjunct included cambia (Obaton, 1960). Limiting rays are also present in other plant families in which an included cambium produces phloem wedges, such as Icacinaceae (Bailey and Howard, 1941; Lens *et al.*, 2008) and some lianas of *Mimosa* (Leguminosae; Angyalossy *et al.*, 2015). Other authors, like Schenck (1893), on the other hand, believed that normal ruptures would be formed periodically at these limiting rays, while new secondary phloem was produced from inside the wedge, given its mechanical fragility. Careful developmental analyses with fresh material have shown, however, that these

ruptures are only artefacts and, hence, non-existent (Ozório-Filho, 2002).

As another possible mechanism to accommodate secondary growth, some Bignonieae develop successive lateral steps on the sides of the original phloem wedges. These steps are formed by portions of cambium on the sides of phloem wedges that switch from regular to variant activity; these steps can be symmetrical, asymmetrical or, more rarely, lacking altogether, with much wider limiting rays present in these cases, such as in *Tanaecium*. While most Bignonieae have asymmetrical phloem steps at the wedges, three genera (two clades), *Cuspidaria* + *Tynanthus*, which together form a clade, and *Manaosella*, exhibit symmetrical phloem wedges. The steps are so conspicuous and regularly spaced in *Tynanthus* species that studies on seasonal formation of xylem show the boundaries of growth rings in the variant xylem of *Tynanthus cognatus* as appearing in a stair-step fashion (Lima *et al.*, 2010). All other features discussed below address the variant secondary phloem in detail.

Phylogenetic and evolutionary comparison of the secondary phloem of Bignonieae

Overall pattern Analysing and comparing the variant secondary phloem of Bignonieae in detail shows us that the phloem in this tribe is extremely diverse; however, two main phloem anatomies can be described (see summary in Fig. 15). The first is illustrated by a stratified structure, with evenly spaced fibre bands, sieve tubes in radial or diffuse arrangement, simple or compound sieve plates with few sieve areas, and abundant intermingling parenchyma. This phloem anatomy is similar to that described for arboreal Bignoniaceae (Roth, 1981) (Fig. 15) and the regular interwedge phloem of Bignonieae (Pace *et al.*, 2011). The other phloem anatomy type in the tribe is described for the first time for the family, being marked by the presence of a background matrix of fibres where all other cell types are embedded, with sieve tubes in tangential arrangement, compound sieve plates with many sieve areas and the axial parenchyma surrounding the sieve tubes (here called 'sieve-tubecentric parenchyma'; Fig. 15).

Diversity and evolution of individual phloem characters

Sieve tube elements in Bignonieae were studied here for their width, sieve plate type, sieve element length, and arrangement. Regarding their width and length, our analyses indicate that sieve tubes are not undergoing directional evolution, towards either an increase or a decrease in their overall size within Bignonieae. This result diverges from the general trend proposed by earlier authors considering sieve tube element length and width on a broader scale, to vascular or seed plants as a whole, which were suggested to undergo a decrease in length and increase in width along time (Hemenway, 1913; Zahur, 1959; Esau, 1969; Den Outer, 1993).

Sieve tube elements in Bignonieae have either simple or compound sieve plates. Two major sister clades within the tribe, the 'Multiples of four extended clade' and the '*Fridericia* and allies extended clade', are marked by a contrasting difference. In the 'Multiples of four extended clade', a reduction in the number of sieve areas per sieve plate is observed along the phylogeny, something confirmed by directional analyses. In contrast, in the '*Fridericia* and allies extended clade' compound

sieve plates with many sieve areas are the most common, with some species bearing >30 sieve areas per sieve plate (e.g. *Pleonotoma tetraquetra*). Compound sieve plates evolving from ancestors with fewer sieve areas is a pattern opposite to that proposed for the angiosperms as a whole (Hemenway, 1913; Esau, 1969). These two sister clades are thought to have split from an ancestral lineage inhabiting lowland Amazon, diversifying in the Amazon and (re)colonizing the Atlantic rainforest (Lohmann *et al.*, 2013). A smaller clade nested within the '*Fridericia* and allies clade', formed by *Fridericia* and *Xylophragma*, occupies the South American dry areas (Lohmann *et al.*, 2013). One could envisage a physiological implication for the compound sieve plates with many sieve areas if *Fridericia* and *Xylophragma* exclusively had this sieve plate type. However, since other species of this clade occupy more moist areas and also have the same anatomical feature, a correlation between habitat occupation and diverse sieve tube element morphologies is debatable.

A few ecological and functional studies have been carried out for phloem, and they did find some correlations between sieve element morphology and environmental or organographic variables. In monocots, simple and supposedly more efficient sieve plates are found in the source organs (i.e. rhizomes full of starch, and leaves), while compound sieve plates are found in sink or consuming organs (i.e. stems and roots; Cheadle and Witford, 1941; Cheadle, 1948). In the eudicot *Styrax*, sieve elements bear transverse and simple sieve plates in the roots and inclined and compound sieve plates in the stem of species growing in the *Cerrado*, a strong seasonally dry environment (Machado *et al.*, 2005, 2007), while always exclusively compound in species growing in more mesic habitats (Machado *et al.*, 2007), suggesting a potential functional role of different sieve plate morphologies. More studies are needed to test possible functional hypotheses.

Meanwhile, the evolutionary significance of sieve area number in the sieve plates remains elusive. We do know that sieve tube elements with simple sieve plates are usually encountered in shorter sieve tube elements, while compound sieve plates are normally found in the longer and wider sieve tube elements (MacDaniels, 1918; Parthasarathy, 1968; Esau, 1969; Den Outer, 1983). This same pattern holds true in Bignonieae, within which the sieve tube elements bearing simple sieve plates are much shorter than those bearing compound sieve plates, an observation confirmed by correlation analyses. In Bignonieae, the presence of shorter sieve tube elements bearing simple sieve plates is additionally associated with the presence of storied structure, as seen in *Perianthomega*, *Amphilophium* and *Dolichandra*. Storied cambia have already been shown to have shorter fusiform initials and, therefore, to produce shorter axial derivatives, both in the xylem and in the phloem (Eames and MacDaniels, 1947; Esau, 1969; Evert, 2006).

Phloem fibres also exhibit contrasting evolutionary patterns within the Bignonieae. In the 'Multiples of four extended clade' we observe a reduction in the abundance of fibres along the phylogeny, while in its sister group, the '*Fridericia* and allies extended clade', the opposite scenario is observed, with an augmentation of fibre abundance, which also holds true for *Stizophyllum* and some species of *Adenocalymma*. The multiple origins for an increase in fibre abundance may be related to the mechanical safety of the conductive cells produced by the

variant cambia within the phloem wedges, similar to what has been proposed for the fibrous secondary phloem of *Carya cordiformis* (Juglandaceae; Eames and MacDaniels, 1947), possibly avoiding damage from natural girdling. Collapse of the sieve tube elements has never been recorded in the phloem of fibrous species, not even in the non-conducting phloem, as opposed to the 'Multiples of four extended clade', where most species experience total collapse of their sieve tube elements in the non-conducting phloem. Evolution towards a decrease in fibre frequency in the 'Multiples of four extended clade', on the other hand, may be enhancing the flexibility of these stems to climb, as some species of this group were suggested as the most flexible in the tribe (e.g. *Dolichandra*; Gentry, 1980). Thus, the combination of lower fibre percentage and multiple phloem wedges (Dos Santos, 1995; Pace *et al.*, 2009) seems to increase stem flexibility, a hypothesis that is currently being tested biomechanically (Gerolamo *et al.*, 2014). The increase in fibre abundance undergone by at least three independent lineages of Bignonieae illustrates the opposite pattern in relation to what had been proposed for the angiosperms as a whole (Hemenway, 1913; Zahur, 1959; Den Outer, 1993), challenging the one-way directionality proposed by these earlier theories. On the other hand, in lineages undergoing an overall decrease in the amount of fibres, we never see their substitution for sclereids in the variant phloem of Bignonieae studied here, contrary to what was predicted by Den Outer (1993), although more studies with different families in which fibres occur are needed to further explore Den Outer's proposal.

Several traits that were variable in Bignonieae have shown an evolutionary correlation with the increase in fibre abundance, such as the tangential arrangement of sieve tube elements, abundant number of sieve areas, the presence of sieve-tubecentric phloem parenchyma and the presence of multiple companion cells. These correlations probably result from architectural constraint (*sensu* Gould and Lewontin, 1979). Bignoniaceae as a whole have a stratified phloem, i.e. a phloem with regularly spaced tangential fibre bands (Roth, 1981; this work). When fibres increase in abundance, these fibre bands become more closely arranged, leading the elements towards tangential disposition, while the axial parenchyma reduces in abundance and becomes sieve-tubecentric. The presence of this sieve-tubecentric axial parenchyma in the fibrous species may contribute fundamentally to phloem transport by creating the osmotic pressure known to be necessary to maintain turgor pressure for phloem loading and unloading (Aloni *et al.*, 1986; Sjölund, 1997; Van Bel, 2003). Also, in some instances functioning integration between the axial parenchyma and the companion cells has been shown, with the parenchyma contributing to the maintenance of sieve elements (Esau, 1969), which may well explain the close association of these cells around the sieve elements in the fibrous species of Bignonieae. A positive correlation was also found between abundant fibres and the presence of more than one companion cell per sieve element. The presence of two companion cells, one lying at each side of the sieve tube element, has already been reported in other plant groups (Cheadle and Esau, 1958; Chavan *et al.*, 1983, 2000). However, the presence of two or three companion cells lying on the same side of the sieve tube element has, to the best of our knowledge, never been mentioned in the literature and may contribute to the maintenance of these long and wide sieve elements in taxa

where a matrix of parenchyma has been substituted for a matrix of fibres. Fibres in Bignonieae as a whole seem to be evolving in a punctuated fashion. When the '*Fridericia* and allies extended clade' is considered alone, phylogenetic statistics indicate that most changes in this lineage occur at the terminal branches, which agrees with a species-specific type of adaptation. Meanwhile, its sister group, the 'Multiples of four extended clade', exhibits the opposite pattern, with most changes occurring early in the evolution of the lineage and with stasis in the terminal branches, a hypothesis consistent with a scenario of ancient diversification.

Other characters encountered in this study were shown to be taxon-specific and therefore diagnostic of some groups, such as the presence of crystalliferous parenchyma sheaths in the 'Multiples of four extended clade' and *Pachyptera*. The presence of crystalliferous parenchyma surrounding the fibre bands is a quite common feature in phloem and has been related to the presence of true fibres (Roth, 1981; Evert, 2006). However, true fibres, differentiating directly from cambial derivatives close to the cambial zone, are found here even in the absence of crystalliferous parenchyma. The multiple origins of different types of crystals and the fact that more than one type of crystal may occur in a single species illustrate how labile might be the conversion of one type of crystallization to another, with the acicular crystals being the most common in this tribe. Crystals have been found in nearly all species, and these have been suggested to play a key role in plant metabolism, being involved in cell division, growth, physiological maintenance and mechanical support (Arnott, 1976; Franceschi, 1989; Marcati and Angyalossy, 2005; Evert, 2006).

CONCLUSIONS

This study shows that the phloem is extremely diverse in the speciose tribe Bignonieae (Bignoniaceae), with two main types of phloem anatomy: a fibrous and a scarcely fibrous phloem (stratified). These different fibre abundances have, in addition, evolved in correlation with sieve elements and axial parenchyma. Ancestral character state reconstructions and phylogenetic statistical analyses have shown that directional evolution of fibre abundance is present in Bignonieae, and with different lineages having evolved in contrasting directions, creating the dissimilar types of phloem anatomy seen today in the tribe. What has likely triggered the appearance in evolution of such contrasting phloem types in Bignonieae remains to be elucidated. Further ecophysiological studies interpreted in the light of the anatomical findings encountered here would be critical in order to address such questions. Moreover, our results challenge the hypotheses of general trends in phloem character evolution, such as decreasing size of the sieve tube elements, increasing sieve tube element diameter, increasing amount of parenchyma and decreasing number of fibres, during angiosperm evolution, which have historically pervaded the anatomical literature. The findings of such contrasting evolutionary patterns even on a narrow taxonomic scale, like the tribe Bignonieae, makes it still more exciting to pursue a holistic understanding of phloem diversification to expand our knowledge on phloem diversification in angiosperms as a whole.

LITERATURE CITED

Aloni B, Wyse RE, Griffith S. 1986. Sucrose transport and phloem unloading in stem of *Vicia faba* – possible involvement of a sucrose carrier and osmotic regulation. *Plant Physiology* **81**: 482–486.

Angyalossy V, Pace MR, Lima AC. 2015. Liana anatomy: a broad perspective on structural evolution of the vascular system. In: SA, Schnitzer, F Bongers, R Burnham, FE Putz, eds. *Ecology of lianas*. Oxford: Wiley-Blackwell.

Angyalossy-Alfonso V, Richter HG. 1991. Wood and bark anatomy of *Buchenavia* Eichl. (Combretaceae). *IAWA Bulletin n.s.* **12**: 123–141.

Arnott H.J. 1976. Calcification in higher plants. In: N Watanabe, KM Wilbur, eds. *The mechanisms of mineralization in the invertebrates and plants*. Columbia: University of South Carolina Press, 55–78.

Bailey IW, Howard RA. 1941. The comparative morphology of the Icacinaceae. I. Anatomy of node and internode. *Journal of the Arnold Arboretum* **22**: 125–132.

Barbosa ACF, Pace MR, Witovisk L, Angyalossy V. 2010. A new method to obtain good anatomical slides of heterogeneous plant parts. *IAWA Journal* **31**: 373–383.

Berlyn GP, Miksche JP. 1976. *Botanical microtechnique and cytochemistry*. Ames: Iowa State University Press.

Bukatsch F. 1972. Bemerkungen zur Doppelfärbung Astrablau-Safranin. *Microkosmos* **61**: 255.

Carlquist S. 1982. The use of ethylenediamine in softening hard plant structures for paraffin sectioning. *Stain Technology* **57**: 311–317.

Carlquist S. 2013. Interxylary phloem: diversity and functions. *Brittonia* **65**: 477–495.

Chattaway M. 1953. The anatomy of bark. I. The genus *Eucalyptus*. *Australian Journal of Botany* **1**: 402–433.

Chavan RR, Shah JJ, Patel KR. 1983. Isolated sieve tube(s)/elements in some angiosperms. *IAWA Bulletin* **4**: 255–263.

Chavan RR, Braggins JE, Harris PJ. 2000. Companion cells in the secondary phloem of Indian dicotyledonous species: a quantitative study. *New Phytologist* **146**: 107–118.

Cheadle VI. 1948. Observations on the phloem in the Monocotyledoneae. II. Additional data on the occurrence and phylogenetic specialization in structure of the sieve tubes in the metaphloem. *American Journal of Botany* **35**: 129–131.

Cheadle VI, Esau K. 1958. Secondary phloem of Calycanthaceae. *University of California Publications – Botany* **29**: 397–510.

Cheadle VI, Whitford NB. 1941. Observations on the phloem in the Monocotyledoneae. I. The occurrence and phylogenetic specialization in structure of the sieve tubes in the metaphloem. *American Journal of Botany* **28**: 623–627.

Cheadle VI, Gifford EM, Esau K. 1953. A staining combination for phloem and contiguous tissues. *Stain Technology* **28**: 49–53.

Costa CG, Coradin VTR, Czarneski CM, Pereira BAS. 1997. Bark anatomy of arborescent Leguminosae of Cerrado and gallery forest of central Brazil. *IAWA Journal* **18**: 385–399.

Den Outer RW. 1983. Comparative study of the secondary phloem of some woody dicotyledons. *Acta Botanica Neerlandica* **32**: 29–38.

Den Outer RW. 1993. Evolutionary trends in secondary phloem anatomy of trees, shrubs and climbers from Africa (mainly Ivory Coast). *Acta Botanica Neerlandica* **42**: 269–287.

Dobbins DR. 1969. Studies on the anomalous cambial activity in *Doxantha unguis-cati* (Bignoniaceae). I. Development of the vascular pattern. *Canadian Journal of Botany* **47**: 2101–2106.

Dobbins DR. 1971. Studies on the anomalous cambial activity in *Doxantha unguis-cati* (Bignoniaceae). II. A case of differential production of secondary tissues. *American Journal of Botany* **58**: 697–705.

Dos Santos GMA. 1995. *Wood anatomy, chloroplast DNA, and flavonoids of the tribe Bignonieae (Bignoniaceae)*. PhD Thesis, University of Reading, UK.

Eames AJ, MacDaniels LH. 1947. *An introduction to plant anatomy*, 2nd edn. New York: McGraw-Hill.

Esau K. 1969. *The phloem*. Berlin: Bornstraeger.

Evert RF. 2006. *Esau's plant anatomy: meristems, cells, and tissues of the plant body – their structure, function, and development*, 3rd edn. New Jersey: Wiley.

Franceschi VR. 1989. Calcium oxalate formation is a rapid and reversible process in *Lemna minor* L. *Protoplasma* **148**: 130–137.

Gentry AH. 1980. Bignoniaceae Part I – tribes Crescentieae and Tourrettieae. *Flora Neotropica*. Monograph 25. New York: New York Botanical Garden Press, 1–130.

Gentry AH. 1991. The distribution and evolution of climbing plants. In: FE Putz, HA Mooney, eds. *The biology of vines*. Cambridge: Cambridge University Press, 3–49.

Gerolamo C, Angeles G, Rowe N, Nogueira A, Angyalossy V. 2014. The impact of cambial variant on the biomechanics and hydraulics of lianas in Bignoniaceae. Poster presented at the International Meeting New Perspectives on Climbing Plants. London: Royal Linnean Society of London.

Gerwing JJ, Schnitzer SA, Burnham RJ, et al. 2006. A standard protocol for liana censuses. *Biotropica* **38**: 256–261.

Gould SJ, Lewontin RC. 1979. The spandrels of San Marco and the Panglossian paradigm: a critique of the adaptationist programme. Proceedings of the Royal Society of London B: Biological Sciences **205**: 581–598.

Hemenway AF. 1911. Studies on the phloem of the dicotyledons I. Phloem of the Juglandaceae. *Botanical Gazette* **51**: 131–135.

Hemenway AF. 1913. Studies on the phloem of the dicotyledons II. The evolution of the sieve-tube – Contributions from the Hull Botanical Laboratory. *Botanical Gazette* **55**: 236–243.

IAWA Committee. 2016. IAWA list of microscopic features for bark research. *IAWA Journal* (in press).

Karnovsky MJ. 1965. A formaldehyde-glutaraldehyde fixative of high osmolality for use in electron microscopy. *Journal of Cell Biology* **27**: 137–138.

Lens F, Kårehed J, Baas P, et al. 2008. The wood anatomy of polyphyletic Icacinaceae *s.l.*, and their relationship within asterids. *Taxon* **57**: 525–552.

Lima AC, Pace MR, Angyalossy V. 2010. Seasonality and growth rings in lianas of Bignoniaceae. *Trees* **24**: 1045–1060.

Lohmann LG. 2006. Untangling the phylogeny of neotropical lianas (Bignonieae, Bignoniaceae). *American Journal of Botany* **93**: 304–318.

Lohmann LG, Taylor CM. 2014. A new generic classification of Bignonieae (Bignoniaceae) based on molecular phylogenetic data and morphological synapomorphies. *Annals of the Missouri Botanical Garden* **99**: 348–489.

Lohmann LG, Bell CD, Calió MF, Winkworth RC. 2013. Pattern and timing of biogeographical history in the Neotropical tribe Bignonieae (Bignoniaceae). *Botanical Journal of the Linnean Society* **171**: 154–170.

MacDaniels LH. 1918. The histology of the phloem in certain woody angiosperms. *American Journal of Botany* **5**: 347–378.

Machado SR, Marcati CR, Morretes BL de, Angyalossy V. 2005. Comparative bark anatomy of root and stem in *Styrax camporum* (Styracaceae). *IAWA Journal* **26**: 477–487.

Machado SR, Rodella RA, Angyalossy V, Marcati CR. 2007. Structural variations in root and stem wood of *Styrax* (Styracaceae) from Brazilian forest and cerrado. *IAWA Journal* **28**: 173–188.

Marcati CR, Angyalossy V. 2005. Seasonal presence of acicular calcium oxalate crystals in the cambial zone of *Citharexylum myrianthum* (Verbenaceae). *IAWA Journal* **26**: 93–98.

Maddison WP, Maddison DR. 2009. Mesquite: a modular system for evolutionary analysis. Version 2.6. http://mesquiteproject.org.

Metcalfe CR, Chalk L. 1950. *Anatomy of the dicotyledons: leaves, stems, and wood in relation to taxonomy with notes on economic uses.* Oxford: Clarendon Press.

Midford P, Maddison WP. 2006. *Pagel 94 analysis module of Mesquite, v1.12.* http://mesquiteproject.org/mesquite/CharacterEvolution/Pagel94.html.

Obaton M. 1960. Les lianes ligneuses a structure anormale des forêts denses d'Afrique Occidentale – Les divers types d'anomalies. *Annales des Sciences Naturelle Botanique et Biologie Végétale* **12**: 20–220.

O'Brien TP, Feder N, McCully ME. 1964. Polychromatic staining of plant cell walls by toluidine blue O. *Protoplasma* **59**: 368–373.

Olmstead RG, Zjhra ML, Lohmann LG, Grose SO, Eckert AJ. 2009. A molecular phylogeny and classification of Bignoniaceae. *American Journal of Botany* **96**: 1731–1743.

Ozório-Filho, HL. 2002. *Variação cambial em Bignoniaceae: padrão anatômico e desenvolvimento do caule.* Masters dissertation, University of São Paulo, Brazil.

Pace MR, Angyalossy V. 2013. Wood anatomy and evolution: a case study in the Bignoniaceae. *International Journal of Plant Sciences* **174**: 1014–1048.

Pace MR, Lohmann LG, Angyalossy V. 2009. The rise and evolution of the cambial variant in Bignonieae (Bignoniaceae). *Evolution and Development* **11**: 465–479.

Pace MR, Lohmann LG, Angyalossy V. 2011. Evolution of disparity between the regular and variant phloem in Bignonieae (Bignoniaceae). *American Journal of Botany* **98**: 602–618.

Pace MR, Lohmann LG, Olmstead RG, Angyalossy V. 2015. Wood anatomy of major Bignoniaceae clades. *Plant Systematics and Evolution* **301**: 967–995.

Pagel MD. 1994. Detecting correlated evolution on phylogenies: a general method for the comparative analysis of discrete characters. *Proceedings of the Royal Society of London B: Biological Sciences* **255**: 37–45.

Pagel MD. 1999. Inferring the historical patterns of biological evolution. *Nature* **401**: 877–884.

Parameswaran N, Liese W. 1970. Mikroskopie der Rinde tropicher Holzarten. In: H Freund, ed. *Handbuch der Mikroskopie in der Technik, Band V, Teil 1,* 2nd edn. Frankfurt: Umschau Verlag, 225–305.

Parthasarathy MV. 1968. Observations on metaphloem in vegetative parts of palms. *American Journal of Botany* **55**: 1140–1168.

Richter HG, Mazzoni-Viveiros SC, Alves ES, Luchi AE, Costa CG. 1996. Padronização de critérios para a descrição anatômica da casca: lista de características e glossário de termos. *IF Série Registros* **16**: 1–25.

Roth I. 1981. Structural patterns of tropical barks. In: HJ Braun, S Carlquist, P Ozenda, I Roth, eds. *Encyclopedia of plant anatomy.* Berlin: Gebrüder Bornstraeger.

Rupp P. 1964. Polyglykol als Einbettungsmedium zum Schneiden botanischer Präparate. *Mikrokosmos* **53**: 123–128.

Schenck H. 1893. Beitrage zur Biologie und Anatomie der Lianen im Besonderen der in Brasilien einheimischen Arten. II. Theil. Beiträge zur Anatomie der Lianen. In: Schimper AFW. *Botanische Mittheilungen aus den Tropen.* Jena: Gustav Fischer.

Schnitzer SA, DeWalt SJ, Chave J 2006. Censuring and measuring lianas: a quantitative comparison of the common methods. *Biotropica* **38**: 581–591.

Sjölund RD. 1997. The phloem sieve element: a river runs through it. *Plant Cell* **9**: 1137–1146.

Solereder H. 1908. Bignoniaceae. In: H Solereder, ed. *Systematic anatomy of the dicotyledon.* Oxford: Clarendon Press, 601–611.

Spangler RE, Olmstead RG. 1999. Phylogenetic analysis of Bignoniaceae based on the cpDNA gene sequences rbcL and ndhF. *Annals of the Missouri Botanical Garden* **86**: 33–46.

Trockenbrodt M. 1990. Survey and discussion of the terminology used in bark anatomy. *IAWA Bulletin n.s.* **11**: 141–166.

Van Bel AJE. 2003. The phloem, a miracle of ingenuity. *Plant Cell and Environment* **26**: 125–149.

Zahur MS. 1959. Comparative study of secondary phloem of 423 species of woody dicotyledons belonging to 85 families. *Cornell University Agricultural Experiment Station Memoir* 358.

APPENDIX

Taxa, collectors and localities. Vouchers for all specimens were deposited in SPF herbarium, unless otherwise indicated after the plant information.

Adenocalymma bracteatum (Cham.) DC., *Castanho 153*, *Lohmann 861*, Rio Negro, Amazonas, Brazil. **Adenocalymma comosum** (Cham.) DC., *Pace 53*, Living collection Plantarum Institute, Nova Odessa, São Paulo, Brazil. **Adenocalymma divaricatum** Miers, *Udulutsch 2808*, Lençóis, Bahia, Brazil. **Adenocalymma flaviflorum** (Miq.) L.G. Lohmann, *Sousa-Baena 2*, Vale do Rio Doce Forest Reserve, Espírito Santo, Brazil. **Adenocalymma neoflavidum** L.G. Lohmann, *Zuntini 23*, Vale do Rio Doce Forest Reserve, Espírito Santo, Brazil. **Adenocalymma nodosum** (Silva Manso) L.G. Lohmann, *Pace 20*, Uberlândia, Minas Gerais, Brazil. **Adenocalymma peregrinum** (Miers) L.G. Lohmann, *Pace 26*, Living collection Plantarum Institute, Nova Odessa, São Paulo, Brazil. **Adenocalymma salmoneum** J.C. Gomes, *Lohmann 658*, Vale do Rio Doce Forest Reserve, Espírito Santo, Brazil. **Adenocalymma tanaeciicarpum** (A.H. Gentry) L.G. Lohmann, *Dos Santos 263*, Porto de Moz, Pará, Brazil, received from the MADw wood collection, vouchers in MAD, MO and MG. **Amphilophium bracteatum** (Cham.) L.G. Lohmann, *Ozório-Filho 8*, São Paulo, São Paulo, Brazil. **Amphilophium crucigerum** (L.) L.G. Lohmann, *Pace 1*, *Pace 2*, *Pace 3*, *Pace 34*, São Paulo, São Paulo, Brazil. **Amphilophium elongatum** (Vahl) L.G. Lohmann, *Pace 45*, Livings collection Plantarum Institute, Nova Odessa, São Paulo, Brazil. **Amphilophium magnoliifolium** (Kunth) L.G. Lohmann, *Lohmann 851*, Rio Negro, Amazonas, Brazil; Dos Santos 272, Porto de Moz, Pará, Brazil, received from the MADw wood collection, vouchers in MAD, MO and MG. **Amphilophium paniculatum** (L.) Kunth, *Pace 46*, Livings collection Plantarum Institute, Nova Odessa, São Paulo, Brazil. **Anemopaegma chamberlaynii** (Sims) Bureau & K. Schum., *Zuntini 15*, Vale do Rio Doce Forest Reserve, Espírito Santo, Brazil. **Anemopaegma laeve** DC., *Pace 338*, Fazenda Bom-Recreio, Boa Nova, Bahia, Brazil. **Anemopaegma robustum** Bureau & K. Schum, *Pace 74*, Reserva Ducke, Manaus, Amazonas, Brazil. **Bignonia binata** Thunb, *Galvanese 22*, Rio Negro, Amazonas, Brazil. **Bignonia campanulata** Cham., *Pace 39*, Livings collection Plantarum Institute, Nova Odessa, São Paulo, Brazil. **Bignonia corymbosa** (Vent.) L.G. Lohmann, *Zuntini 2*, *Zuntini 17*, Vale do Rio Doce Forest Reserve, Espírito Santo, Brazil. **Bignonia magnifica** W. Bull, *Pace 51*, Livings collection Plantarum Institute, Nova Odessa, São Paulo, Brazil. **Bignonia prieurei** DC., *Zuntini 13*, Vale do Rio Doce Forest Reserve, Espírito Santo, Brazil. **Callichlamys latifolia** (Rich.) K. Schum, *Zuntini 175*, Vale do Rio Doce Forest Reserve, Espírito Santo, Brazil.; *Pace 42* Livings collection Plantarum Institute, Nova Odessa, São Paulo, Brazil; *Pace 63*, Reserva Ducke, Manaus, Amazonas, Brazil. **Cuspidaria convoluta** (Vell.) A.H. Gentry, *Pace 48* Living collection Plantarum Institute, Nova Odessa, São Paulo, Brazil. **Cuspidaria pulchra** (Cham.) L.G. Lohmann, *Pace 24*, *Pace 25*, Uberlândia, Minas Gerais, Brazil. **Dolichandra quadrivalvis** (Jacq.) L.G.

Lohmann, *Pace 105*, Corumbá, Mato Grosso do Sul, Brazil. ***Dolichandra unguiculata*** (Vell.) L.G. Lohmann, *Zuntini 176*, Vale do Rio Doce Forest Reserve, Espírito Santo, Brazil. ***Dolichandra unguis-cati*** (L.) L.G. Lohmann, *Ceccantini 2687*, Matozinhos, Minas Gerais, Brazil; *Groppo 322*, São Paulo, São Paulo, Brazil. ***Fridericia chica*** (Bonpl.) L.G. Lohmann, *Pace 50*, Livings collection Plantarum Institute, Nova Odessa, São Paulo, Brazil. ***Fridericia conjugata*** (Vell.) L.G. Lohmann, *Pace 44*, Livings collection Plantarum Institute, Nova Odessa, São Paulo, Brazil. ***Fridericia platyphylla*** (Cham.) L.G. Lohmann, *Pace 22*, *Pace 23*, Uberlândia, Minas Gerais, Brazil. ***Fridericia samydoides*** (Cham.) L.G. Lohmann, *Pace 49*, Livings collection Plantarum Institute, Nova Odessa, São Paulo, Brazil. ***Fridericia speciosa*** Mart., *Pace 40*, Livings collection Plantarum Institute, Nova Odessa, São Paulo, Brazil. ***Lundia damazioi*** C. DC., *Pace 55*, *Pace 56*, São Paulo, São Paulo, Brazil. ***Lundia longa*** (Vell.) DC., *Zuntini 1*, Vale do Rio Doce Forest Reserve, Espírito Santo, Brazil; *Pace 227*, Reserva Biológica de Poço das Antas, Silva Jardim, Rio de Janeiro, Brazil. ***Manaosella cordifolia*** (DC.) A.H. Gentry, *Pace 41*, Brazil, Livings collection Plantarum Institute, Nova Odessa, São Paulo, Brazil. ***Mansoa difficilis*** (Cham.) Bureau & K. Schum., *Pace 35*, São Paulo, São Paulo, Brazil; *Zuntini 4*, Vale do Rio Doce Forest Reserve, Espírito Santo, Brazil. ***Mansoa onohualcoides*** A.H. Gentry, *Zuntini 276*, Vale do Rio Doce Forest Reserve, Espírito Santo, Brazil. ***Mansoa standleyi*** (Steyerm.) A.H. Gentry, *Pace 43*, Livings collection Plantarum Institute, Nova Odessa, São Paulo, Brazil. ***Martinella obovata*** (Kunth) Bureau & K. Schum., *Zuntini 7*, Vale do Rio Doce Forest Reserve, Espírito Santo, Brazil; *Dos Santos 237*, Porto de Moz, Xingu riverside, Pará, Brazil, analysed at MADw wood collection, voucher in MAD, MO, MG; Dos Santos 317, Gurupa, Moju riverside, tributary of the Amazon River, Pará, Brazil, analysed at MADw, voucher in MAD, MO, MG. ***Neojobertia mirabilis*** (Sandwith) L.G. Lohmann, *Dos Santos 48*, Buriticupu Forest Reserve, Maranhão, Brazil, received from the MADw wood collection, vouchers in the MAD, MO, and MG. ***Neojobertia* sp. nov.**, *Zuntini 18*, Vale do Rio Doce Forest Reserve, Espírito Santo, Brazil. ***Pachyptera kerere*** (Aubl.) Sandwith, *Castanho 143*, *Lohmann 834*, Rio Negro, Amazonas, Brazil. ***Perianthomega vellozoi*** Bureau, *Pace 10*, *Pace 15*, Viçosa, Minas Gerais, Brazil; *Pace 28*, *Pace 29*, Santa Cruz de la Sierra, Santa Cruz, Bolivia. ***Pleonotoma albiflora*** (Salzm. ex DC.) A.H. Gentry, *Pace 78*, Reserva Ducke, Manaus, Amazonas, Brazil. ***Pleonotoma tetraquetra*** (Cham.) Bureau, *Ozório-Filho 11*, São Paulo, São Paulo, Brazil. ***Pleonotoma stichadenia*** K. Schum., *Zuntini 7*, Vale do Rio Doce Forest Reserve, Espírito Santo, Brazil; *Dos Santos 187*, Parauapebas, Pará, Brazil, analysed at the MADw wood collection, vouchers in MAD, MO and MG. ***Pyrostegia venusta*** (Ker Gawl.) Miers, *Pace 17*, Campinas, São Paulo, Brazil; *Pace 36*, São Paulo, São Paulo, Brazil. ***Stizophyllum riparium*** (Kunth) Sandwith, *Pace 16*, *Pace 33*, São Paulo, São Paulo, Brazil; *Zuntini 9*, Vale do Rio Doce Forest Reserve, Espírito Santo, Brazil. ***Tanaecium bilabiatum*** (Sprague) L.G. Lohmann, *Lohmann 850*, Rio Negro Amazonas, Brazil. ***Tanaecium pyramidatum*** (Rich.) L.G. Lohmann, *Pace 14*, *Pace 35*, São Paulo, São Paulo, Brazil. ***Tynanthus cognatus*** (Cham.) Miers: *Pace 9a*, *Pace 9b*, São Paulo, São Paulo, Brazil. ***Tynanthus elegans*** Miers, *Zuntini 147*, Vale do Rio Doce Forest Reserve, Espírito Santo, Brazil. ***Xylophragma myrianthum*** (Cham. ex Steud.) Sprague.